

## Global stability of spiral flow

By D. D. JOSEPH AND B. R. MUNSON†

Department of Aerospace Engineering and Mechanics,  
University of Minnesota, Minneapolis 55455

(Received 4 November 1969)

Energy and linear limits are calculated for the Poiseuille–Couette spiral motion between concentric cylinders which rotate rigidly and rotate and slide relative to one another. The addition of solid rotation can bring the linear limit down to the energy limit with coincidence achieved in the limit of infinitely fast rotation. If the differential rotation is also added, the solid rotation rate need be only finite to achieve near coincidence. Sufficient conditions for non-existence of sub-linear instability are derived. The basic spiral character of the instability is analysed and the results compared with the experiments of Ludwig (1964).

### 1. Introduction

The basic motion whose stability will be studied is a spiral flow between concentric rotating sliding cylinders. Forward motion is induced by the shear of sliding the cylinders relative to one another and by a uniform pressure gradient along the pipe axis. Circumferential flow is induced by the shear transmitted by a differential rotation. The basic flow is, therefore, a combination of Couette and Poiseuille flow between annular cylinders; it does not involve inertial non-linearities and is independent of the flow Reynolds number.

These annular flows are simple enough to allow analysis, yet they do contain a domain parameter, the radius ratio, which allows one to see how the stability limits change as the domain is varied from the round pipe to the (narrow-gap) channel. The variation of the stability and instability limits with the radius ratio is a valuable and sensitive experimental observable, which seems to have received almost no theoretical attention.‡

The theoretical context of our study of spiral flow is a global theory in which the linear limit gives sufficient conditions for instability, and the energy limit gives sufficient conditions for stability (for example, Joseph 1966, Joseph & Shir 1967). When the two limits coincide, they define the necessary and sufficient condition for stability. Ordinarily, these two limits will not coincide. Then, the region between the two limits is a candidate for non-linear instability. We call such non-linear instability which lies below the linear limit ‘sublinear’.

† Present address: Department of Mechanical Engineering, Duke University, Durham, North Carolina.

‡ But the domain variations are studied in Couette flow between rotating cylinders by Sparrow, Munro & Jonsson (1964) and by Nickerson (1969), and in Poiseuille flow by Mott & Joseph (1968) and Joseph & Carmi (1969).

In shear flow, sublinear instability seems to be the rule rather than exception, and even in boundary layers, it seems possible to initiate transition at Reynolds numbers far below the ones for which the Tollmein–Schlichting waves appear (Elder 1960). For Poiseuille and Couette flow, the energy limits and linear limits are very far apart, and neither is ‘close’ to experiment (Joseph & Carmi 1969).

The addition of rotation even without differential rotation can strongly alter this stability picture. With differential rotation, one can have Rayleigh’s central force mechanism as a source for instability, and the possibility of some type of Taylor vortex disturbance must be considered. But even a ‘stabilizing’ distribution of angular momentum (increasing outward) can (and does) provide an environment in which disturbance Coriolis forces can exist and induce instability. The essentially inviscid character of these forces associated with rotation make attractive an entirely inviscid analysis of the stability problem, and such analyses have been constructed by Chandrasekhar (1960) and Howard & Gupta (1962) in the restricted context of axially-symmetric disturbances. But the really interesting deep (low Reynolds number) instabilities, which one might expect to be associated with axially-symmetric Taylor vortices when the flow is pure swirl, it turns out, are associated with a spiral when the flow is a spiral. This was shown, first, by the inviscid analysis of Ludwig (1961) and, later, by a most ingenious experiment (Ludwig 1964) which gives to this spiral flow a very central place in the theory of hydrodynamic stability. It is now clear from the work of Pedley (1968) that the result of Ludwig does not depend in any profound way on the choice of a particular (linear shear) velocity profile.

Of course, one cannot tell from inviscid analysis whether an instability is deep. For this we need the criterion for stability and, even in the context of a linearized theory, this requires a Reynolds number. One aim of the paper is a linear theory for Ludwig’s experiment which could also be used for future experiments with spiral flow. For the narrow gap, such an analysis is already partly available in the paper of Kiessling (1963). But apart from a special (Bénard problem) solution which does not give the smallest linear limit, Kiessling is forced to approximate the solution with a Galerkin iterative procedure, which seems not to converge well for all of the values of the parameters considered by him. We have given a much simpler linear analysis, not so much for the above reasons, but because Kiessling’s results are not extensive enough to allow for a comparison with the result of energy analysis or with experiments.

The analyses of Taylor flow between cylinders with small axial (Poiseuille) flow of Hughes & Reid (1968), Krueger & Di Prima (1964) and Datta (1965) have a somewhat special character, because they allow only for axisymmetric disturbances, and these are not the most unstable.

Linear viscous analyses for the rotating Couette and Poiseuille flow do already demonstrate profound rotation-induced changes which, for suitably adjusted rates of rigid rotation, drive the stationary, absolutely-stable pipe and Couette flow to instability at Reynolds numbers of about 100.

What is even more remarkable is that the rotation can drive the linear limit so low that it can be brought into exact, or nearly exact, coincidence with the (rotation-free) energy limit. At any rate, for some parameter values, the strongest

possible stability statements (which imply extremely rapid decay of disturbance of any size) can be given. The fact that this coincidence of the stability and instability limits could be achieved in a rotating plane Couette flow was first observed to be true by Busse (private communication). The fact that the same coincidence can be achieved in a rapidly rotating parabolic Poiseuille flow is noted in the paper of Joseph & Carmi (1969).

This study develops the most general conditions under which the exact spiral-flow solutions of the Navier–Stokes equations are sublinearly stable, or nearly so. Our results hold for logarithmic or parabolic axial profiles in Couette or combined Couette–Poiseuille flow between sliding and rotating concentric cylinders. The main result is this: At all radius ratios (except for small ones, say  $\eta > 0.1$ ), one can define a mean, basic-flow spiral angle and an energy spiral angle. The energy functional takes on its maximum value among functions which do not vary along the energy spiral. It is possible, for every spiral angle and radius ratio, to choose a rotating co-ordinate system in which the disturbance exists and is steady, and to choose a differential rotation to make the energy and basic-flow spiral coincide. Then, the energy and linear limits coincide (nearly for most parameters, exactly for others). Stated in another way: the problem of spiral flow is characterized by an axial speed, an angular-velocity difference, an angular velocity and the radius ratio. It is possible to specify, *a priori*, an explicit relation among these four parameters to bring the instability and stability limits into coincidence or near coincidence.

Without the optimal adjustment of the differential rotation, our analysis indicates that one can still find a rotating co-ordinate system in which the disturbance is steady, but the disturbance spiral and energy spiral (basic-flow spiral) do not, then, coincide. For these cases, a region where sublinear solutions must occur, if they exist, is delineated.

The analysis allows proof of what has been said within a mean-radius approximation and, without this approximation, in several limiting cases.

To the considerable extent to which the outcome of this analysis can be compared with the experimental results of Ludwig, the agreement is good.

Not all of our results are established rigorously. Rigorous results are given as lemmas and theorems.

## 2. The basic-spiral motion

Let  $R_1$ ,  $\Omega_1$  and  $R_2$ ,  $\Omega_2$  be the radii and constant angular velocity, respectively, of the inner and outer cylinders. The cylinders are pulled axially so that the difference in axial speed is  $U_c$ , and the co-ordinate system is chosen so that the inner and outer cylinders have axial speeds  $U_c$  and 0, respectively. An axial pressure gradient is maintained so that the maximum excess axial speed above that induced by sliding is  $U_p$ . The physical problem and co-ordinates are sketched in figure 1.

Let  $(R, \phi, X)$  be the polar cylindrical co-ordinates and  $R_1 \leq R \leq R_2$ ,  $\eta = R_1/R_2$ . A basic laminar solution of the Navier–Stokes equations of the form

$$(U_R, U'_\phi, U_X) = (0, U'_\phi(R), U_X(R))$$

is readily obtained as

$$U'_\phi = AR + B/R, \tag{2.1}$$

$$A = \frac{R_2^2 \Omega_2 - R_1^2 \Omega_1}{R_2^2 - R_1^2}, \quad B = -\frac{R_2^2 R_1^2 (\Omega_2 - \Omega_1)}{R_2^2 - R_1^2},$$

and

$$U_X = U_p \left\{ \frac{1 - (R/R_2)^2 + (\eta^2 - 1) \ln(R/R_2)/\ln \eta}{1 - (\eta^2 - 1) + (\eta^2 - 1) \ln[(\eta^2 - 1)/\ln \eta^2]/\ln \eta^2} \right\} + U_c \ln(R/R_2)/\ln \eta. \tag{2.2}$$

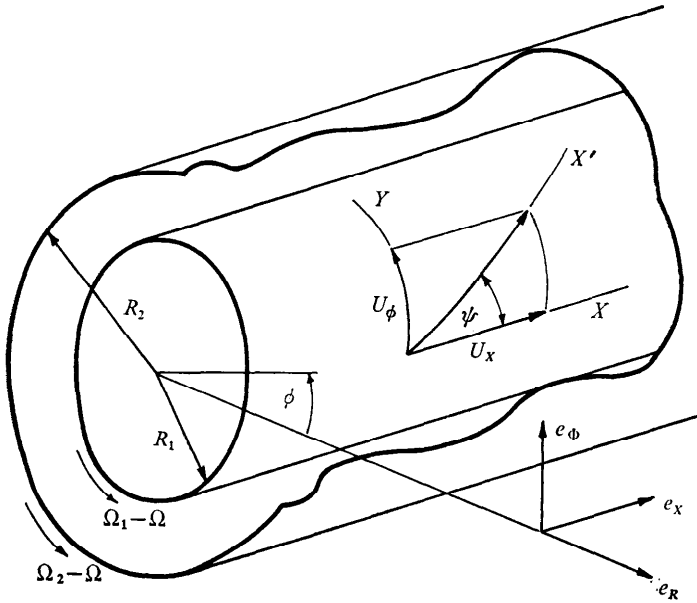


FIGURE 1. Spiral flow between rotating-sliding cylinders. Basic flow:  $\mathbf{U} = (0, U_\phi(R), U_R(R))$ . Disturbance flow:  $\mathbf{u} = (w, v, u)$ .

$U_p$  is the maximum value ( $R/R_2 = [(\eta^2 - 1)/\ln \eta^2]^{\frac{1}{2}}$ ) of the part of the velocity which is forced by the axial pressure gradient alone. We are able to get especially interesting results when  $U_x$  has one of two special forms. The first of these is Couette flow ( $U_p = 0$ ), and the second is the parabolic flow

$$U_X = U_q(1 - R^2/R_2^2) \tag{2.3}$$

which is obtained from (2.2) by properly relating  $U_p$  and  $U_c$ .

In the work, it is convenient to express the velocity components relative to a co-ordinate system which rotates with a constant angular velocity  $\Omega$ . In this rotating system, (2.2) is unchanged, but (2.1) becomes

$$U_\phi = (\Omega_2 - \Omega) R + \frac{\eta R_1 (\Omega_2 - \Omega_1) [(R/R_2)^2 - 1]}{(1 - \eta^2) R/R_2}. \tag{2.4}$$

The vector  $\mathbf{U}$  is the velocity relative to the rotating co-ordinates.

Many of the classical stability problems are special cases of spiral flow. When  $U_p = 0$ , (2.2) describes Couette flow between rotating and sliding cylinders. If the velocity  $U_c$  of sliding is zero, one has the well-known problem of Couette flow

between rotating cylinders leading to instability in the form of Taylor vortices. In the limit  $\eta \rightarrow 1$ , we recover the problem in which the plane Couette flow rotates around an angular-velocity vector in a plane parallel to the boundaries but oblique to the relative motion of the boundaries. With  $U_c = \Omega_1 = \Omega_2 = 0$ , we have classical Poiseuille flow in a channel ( $\eta = 1$ ) or a pipe ( $\eta = 0$ ) or in an annulus.

Dimensionless co-ordinates are  $(r, \phi, x)$ , where the unit of length is  $R_2 - R_1$  and  $R/R_2 = r(1 - \eta)$ . The basic flow velocities are made dimensionless with a reference velocity  $U_0$  (to be specified later), and the dimensionless velocity components are  $(0, V, U)$ , where  $V(r)$  is the dimensionless version of (2.4). The Reynolds number is taken as  $U_0(R_2 - R_1)/\nu$ . For the disturbance, we shall use the velocity vector  $\mathbf{u}$  with components  $(u, v, w)$ . We use the same notation  $\mathbf{u}, u, v, w$  for the physical disturbance, the dimensionless disturbance or the amplitude of the normal-mode decomposition of this disturbance. The meanings of the symbols will be clear from the context in which they are used.

### 3. Stability and instability equations for spiral flow

The analysis starts from the non-linear Navier–Stokes equations written relative to a system of co-ordinates rotating with a steady angular velocity:

$$\frac{\partial \mathbf{u}}{\partial t} + 2\boldsymbol{\Omega} \times \mathbf{u} + (\mathbf{u} \cdot \nabla) \mathbf{u} + (\mathbf{u} \cdot \nabla) \mathbf{U} + (\mathbf{U} \cdot \nabla) \mathbf{u} = -\nabla p + \nu \Delta \mathbf{u}, \tag{3.1}$$

$$\nabla \cdot \mathbf{u} = 0, \quad \mathbf{u}(X, Y, Z) = \mathbf{u}(X + 2\pi/\alpha, Y, Z), \tag{3.2a, b}$$

and 
$$\mathbf{u} = 0|_{R=R_1, R_2}. \tag{3.2c}$$

Here, for  $\mathbf{U}$  we understand the spiral flow of the previous section.

Let  $\langle \rangle$  designate integration over a volume of pipe of length  $2\pi/\alpha$ . Multiplication of (3.1) by  $\mathbf{u}$  followed by  $\langle \rangle$  using (3.2) gives (see Serrin 1959 or Joseph 1966)

$$\frac{1}{2} \frac{d}{dt} \langle |\mathbf{u}|^2 \rangle + \langle \mathbf{u} \cdot \nabla \mathbf{U} \cdot \mathbf{u} \rangle = -\nu \langle \nabla \mathbf{u} : \nabla \mathbf{u} \rangle. \tag{3.3}$$

The form of this equation is independent of the rigid rotation, for though  $\mathbf{U}$  depends on  $\boldsymbol{\Omega}$ , the symmetric form  $\mathbf{u} \cdot \nabla \mathbf{U} \cdot \mathbf{u}$  does not.

As in Joseph (1966),

$$\frac{1}{2} \frac{d}{dt} \langle |\mathbf{u}|^2 \rangle = \langle |\nabla \mathbf{u}|^2 \rangle \left\{ -\frac{\langle \mathbf{u} \cdot \nabla \mathbf{U} \cdot \mathbf{u} \rangle}{\langle |\nabla \mathbf{u}|^2 \rangle} - \nu \right\} \leq -a^2(\nu - \nu_E) \langle |\mathbf{u}|^2 \rangle.$$

Here,  $\langle |\nabla \mathbf{u}|^2 \rangle \geq a^2 \langle |\mathbf{u}|^2 \rangle$  and  $\nu > \nu_E$  where

$$\nu_E = \max_A \{ -\langle \mathbf{u} \cdot \nabla \mathbf{U} \cdot \mathbf{u} \rangle / \langle |\nabla \mathbf{u}|^2 \rangle \}, \tag{3.4}$$

and  $\mathcal{A}$  is the collection of smooth functions satisfying (3.2). Then,

$$\frac{1}{2} \langle |\mathbf{u}|^2 \rangle \leq \frac{1}{2} \langle |\mathbf{u}|^2 \rangle|_{t=0} \exp \{ 2a^2(\nu_E - \nu) t \}. \tag{3.5}$$

It follows that if  $\nu_E < \nu$ , the motion  $\mathbf{U}$  is stable and any disturbance of this motion decays very fast. On the other hand, if  $\nu < \nu_E$ , an initial disturbance can be found which will make the energy increase for a time. For example, the

disturbance which solves (3.4) will make  $\langle |\mathbf{u}|^2 \rangle$  increase if  $\nu < \nu_E$ . This can be seen by inspection of (3.3).

The energy criterion  $\nu_E < \nu$  suffices to guarantee stability. We obtain the energy limit  $\nu_E$  as the largest of the eigenvalues  $\delta$  of the Euler equations

$$\mathcal{D}' \cdot \mathbf{u} = \delta \Delta \mathbf{u} - \nabla p^* \tag{3.6}$$

for (3.4). Here  $\mathcal{D}'$ , the symmetric part of  $\nabla \mathbf{U}$ , is the rate of strain matrix. The rotation parameters  $\Omega_1$  and  $\Omega_2$  can enter  $\mathcal{D}$  only in the combination  $\Omega_2 - \Omega_1$ . In dimensionless variables ( $U_0$  is the unit of velocity and  $R_2 - R_1$  is the unit of length,  $\rho_E \sim U_0(R_2 - R_1)/\nu$ )

$$\rho_E \mathcal{D} \cdot \mathbf{u} = \Delta \mathbf{u} - \nabla P, \tag{3.7}$$

where 
$$\mathcal{D} \cdot \mathbf{u} = \frac{R_2 - R_1}{2U_0} \begin{bmatrix} vr\bar{D}(U_\phi/R) + u\bar{D}U_X \\ wR\bar{D}(U_\phi/R) \\ w\bar{D}U_X \end{bmatrix} \equiv \frac{1}{2} \begin{bmatrix} vrD(V/r) + uDU \\ wD(V/r) \\ wDU \end{bmatrix},$$

and  $\bar{D} = d/dR, D = d/dr$ .

The linear problem for (3.1) (put  $(\mathbf{u} \cdot \nabla) \mathbf{u} = 0$ ) gives a linear limit  $\nu = \nu_L$  and a criterion  $\nu_L > \nu$  which is sufficient for the instability of (3.1), (3.2) (cf. §6). The linear limit depends on the rotation parameters  $\Omega_1$  and  $\Omega_2$ , independently. Hence, the linear limit depends on one more parameter than the energy limit, and we want to learn how to choose this parameter to give the deepest instability (§§6, 7).

#### 4. Energy (stability) eigenvalue problem

It is, in general, not possible to solve the stability or instability problem for spiral flow exactly (but it can be done when  $U_p = 0$  and  $\eta \rightarrow 1$ ). It is possible, nevertheless, to establish a few important analytical results. These are: (1) symmetry requirements which both establish a basic asymmetry for spiral flow and reduce the range of parameter values over which the search must be carried out, (2) eigenvalue estimates which assure the existence of an extremalizing wave-number with a finite, non-zero modulus, and (3) at the same time, give bounds on the stability and instability limits.

Equation (3.7) can be reduced by normal modes proportional to  $\exp\{i(\alpha x + n\phi)\}$ , where  $n$  ranges over integers. This leads to the eigenvalue problem for the eigenvalues  $\rho_E$

$$\left. \begin{aligned} \frac{1}{2}\rho_E vrD(V/r) + \frac{1}{2}\rho_E uDU &= \mathcal{L}_n w - (2in/r^2)v - Dp, \\ \frac{1}{2}\rho_E wrD(V/r) &= \mathcal{L}_n v + (2in/r^2)w - inp/r, \\ \frac{1}{2}\rho_E wDU &= L_n u - i\alpha p, \end{aligned} \right\} \tag{4.1}$$

$$D(wr) + inv + i\alpha ru = 0,$$

where 
$$\mathbf{u} = v = w = 0|_{r=(1-\eta)^{-1}, \eta(1-\eta)^{-1}} \tag{4.2}$$

$$\mathcal{L}_n = \frac{1}{r}D(rD) - \frac{n^2 + 1}{r^2} - \alpha^2, \quad L_n \equiv \mathcal{L}_n + \frac{1}{r^2} \equiv L.$$

The working equations for the calculations are obtained from (4.1) as follows: Set  $\ell = wr$ , eliminate  $p$  and  $v$  from (4.1) to find

$$-\frac{1}{2}\rho_E n^2 u(DU)/r - (\alpha^2 L\ell + 2i\alpha^3 u + i\alpha r D L u) + \frac{1}{2}\rho_E n\{\alpha r u D(V/r) - (i\ell/r) D(rD(V/r)) - 2iD\ell D(V/r)\} = L^2\ell + 4i\alpha L u, \quad (4.3)$$

and

$$-\frac{1}{2}\rho_E n^2 \ell(DU)/r = i\alpha r D L \ell - (n^2 + \alpha^2 r^2) L u - 2\alpha^2 r D u - \frac{1}{2}\rho_E \alpha n \ell r D(V/r). \quad (4.4)$$

The basic working equations are (4.4) and the following

$$\begin{aligned} &-\frac{1}{2}\rho_E r^{-1} D U \{(n^2 + \alpha^2 r^2) u + i\alpha r D \ell\} - i\alpha r \ell D(r^{-1} D U) \\ &+ \frac{1}{2}\rho_E \{(\alpha/n)(n^2 + \alpha^2 r^2) u r D(V/r) - (in/r) \ell D(rD(V/r)) \\ &- (in/r)(2n^2 + \alpha^2 r^2) D \ell r D(V/r)\} = L^2 \ell + 4i\alpha u, \end{aligned} \quad (4.5)$$

which is obtained from (4.3), (4.4). At the boundary,  $r = \eta/(1 - \eta)$  and  $1/(1 - \eta)$ ,

$$u = \ell = D\ell = 0. \quad (4.6)$$

The system (4.4), (4.5), (4.6) is an eigenvalue problem for the numbers  $\rho_E(U, V, \alpha, n)$ . This system is equivalent to (4.1), (4.2) and determines the same eigenvalues and eigenfunctions. We search over functions  $u$  and  $\ell$  and numbers  $\alpha$  and  $n$  for the smallest of the values  $\rho_E(U, V, \alpha, n)$ .

Symmetry properties of  $\rho_E$  are the subject of the following:

LEMMA 1. Let  $\rho_E(U, V, \alpha, n)$  be any eigenvalue of (4.1), (4.2). Then

$$\begin{aligned} \rho_E(U, V, \alpha, n) &= \rho_E(-U, V, -\alpha, n) = \rho_E(-U, V, \alpha, -n) \\ &= \rho_E(U, -V, -\alpha, n) = \rho_E(U, -V, \alpha, -n) = \rho_E(U, V, -\alpha, -n). \end{aligned} \quad (4.7)$$

The eigenvalue is unchanged if the ratio of ratios  $U/V$  to  $\alpha/n$  is of one sign. If either  $U$  or  $V$  is zero, then we have complete symmetry with respect to  $\alpha$  and  $n$ . It is an interesting mathematical (and physical) fact that the spiral flow has not complete symmetry but, instead, is characterized by the ‘screw’ symmetry just mentioned.

*Proof of Lemma 1*

Let  $u, \ell$  be the eigenfunction for (4.4), (4.5), (4.6) with eigenvalue  $\rho_E(U, V, \alpha, n)$ . Then, the following transformations leave (4.4), (4.5), (4.6) unchanged:

- (1)  $U, \alpha \rightarrow -U, -\alpha; \quad u, \ell \rightarrow -u, \ell,$
- (2)  $U, n \rightarrow -U, -n; \quad u, \ell \rightarrow -u^*, \ell^*,$
- (3)  $V, \alpha \rightarrow -V, -\alpha; \quad u, \ell \rightarrow u^*, \ell^*,$
- (4)  $V, n \rightarrow -V, -n; \quad u, \ell \rightarrow u, \ell^*,$
- (5)  $\alpha, n \rightarrow -\alpha, -n; \quad u, \ell \rightarrow u^*, \ell^*,$

where an asterisk denotes complex conjugates. The eigenfunctions on the right determine the last five eigenvalues of (4.7), respectively. The lemma shows that we can restrict the search for the smallest eigenvalue  $\rho_E$  to a half-plane, say

$$n \geq 0, \quad -\infty < \alpha < \infty.$$

We shall show, in lemma 3, that the required minimum can be found in the finite half-plane away from the origin. In this way, we exclude the possibility that  $\rho_E$  takes on its smallest values as  $\alpha^2 + n^2 \rightarrow 0$  or  $\alpha^2 + n^2 \rightarrow \infty$ . We need first, however, to give a family of isoperimetric inequalities involving Bessel functions.

**LEMMA 2.** *The solution of the minimum problem*

$$\lambda(l, \eta) = \min \int_{\eta}^1 R(du/dR)^2 dR / \int_{\eta}^1 R^{l+1} u^2 dR \tag{4.8}$$

among functions  $u(R)$  which vanish at  $R = \eta$  and  $R = 1$  is ( $l \neq -2$ )

$$\lambda(l, \eta) = \left(\frac{2+l}{2}\right)^2 \lambda(0, \eta^{\frac{1}{2}(2+l)}), \tag{4.9}$$

where  $\lambda(0, \eta)$  is found as the first positive root of the equation

$$0 = J_0(\lambda^{\frac{1}{2}} \eta) Y_0(\lambda^{\frac{1}{2}}) - J_0(\lambda^{\frac{1}{2}}) Y_0(\lambda^{\frac{1}{2}} \eta),$$

and

$$\lambda(-2, \eta) = \pi^2 / (\ln \eta)^2. \tag{4.10}$$

*Proof of Lemma 2*

Under the transformation  $y = R^{1+l/2}$ , we can write

$$\hat{\lambda} = \frac{\int_{\eta}^1 R(du/dR)^2 dR}{\int_{\eta}^1 R^{l+1} u^2 dR} = \left(\frac{2+l}{2}\right)^2 \frac{\int_{\eta^{1+l/2}}^1 y(du/dy)^2 dy}{\int_{\eta^{1+l/2}}^1 y u^2 dy} \equiv \left(\frac{2+l}{2}\right)^2 \hat{\lambda}(0, \eta^{1+l/2}).$$

The Euler equation for the minimum of the functional  $\hat{\lambda}(0, \eta^{1+l/2})$  is

$$\left. \begin{aligned} \frac{1}{y} \frac{d}{dy} \left( y \frac{du}{dy} \right) + \hat{\lambda} u &= 0, \\ u(R(y)) &= 0 \quad \text{at } y = 1, \eta^{1+l/2}. \end{aligned} \right\} \tag{4.11}$$

The solution of this problem is the Bessel function

$$u(y, \eta) = J_0(\hat{\lambda}^{\frac{1}{2}} y) Y_0(\hat{\lambda}^{\frac{1}{2}} \eta^{1+l/2}) - J_0(\hat{\lambda}^{\frac{1}{2}} \eta^{1+l/2}) Y_0(\hat{\lambda}^{\frac{1}{2}} y).$$

This vanishes for  $y = 1$  if  $\hat{\lambda}$  is a zero of  $u(1, \eta)$ . The smallest positive root  $\hat{\lambda} = \lambda$  is the solution of the minimum problem (4.8).

If  $l = -2$ , the transformation  $y = R^{1+l/2}$  breaks down, and we work directly with the Euler equation for the functional  $\hat{\lambda}(-2, \eta)$ . This is

$$\begin{aligned} \frac{1}{R} \frac{d}{dR} \left( R \frac{du}{dR} \right) + \hat{\lambda} \frac{u}{R^2} &= 0, \\ u(1) &= u(\eta) = 0. \end{aligned}$$

The general solution is

$$u = A \cos(\hat{\lambda}^{\frac{1}{2}} \ln R) + B \sin(\hat{\lambda}^{\frac{1}{2}} \ln R).$$

To satisfy the boundary conditions, we must have

$$\hat{\lambda} = \frac{m^2 \pi^2}{(\ln \eta)^2} \quad (m = 1, 2, \dots).$$

The smallest value  $\lambda$  of  $\hat{\lambda}$  is given when  $m = 1$ .



On the range  $\eta/(1-\eta) \leq r \leq 1/(1-\eta)$ , we may write the isoperimetric inequalities as

$$\langle |Du|^2 \rangle \geq (1-\eta)^{l+2} \lambda(l, \eta) \langle r^l |u|^2 \rangle \tag{4.12}$$

and

$$\langle |Du|^2 \rangle \geq \frac{\pi^2}{(\ln \eta)^2} \left\langle \left| \frac{u}{r} \right|^2 \right\rangle, \tag{4.13}$$

where

$$\langle \cdot \rangle = \int_{\eta/(1-\eta)}^{1/(1-\eta)} \cdot r \, dr.$$

With these inequalities, we can locate the minimum of  $\rho_E$  in the finite half  $(\alpha, n)$  plane away from the origin, and, at the same time, give a preliminary estimate of the limit for strong exponential stability.

LEMMA 3. Let  $\rho_E(U, V, \alpha, n, \eta)$  be any eigenvalue of (4.1), (4.2) where  $\alpha$  and  $n$  are any real numbers and  $0 \leq \eta \leq 1$ . Then

$$1/\rho_E \leq \min [m_1, m_2], \tag{4.14}$$

where

$$m_1 = \frac{1}{2}(a_1 + a_2 + a_3), \quad m_2 = (a_4 + a_5 + a_6) \{ \alpha^2 + (1-\eta)^2 n^2 \}^{\frac{1}{2}},$$

$$a_1 = \frac{2\eta |R_1(\Omega_1 - \Omega_2)/U_0|/(1+\eta)}{\{ [\pi^2(1-\eta)^2/(\ln \eta)^2] + \alpha^2 \eta^2 + (1-\eta)^2 (n-1)^2 \}},$$

$$a_2 = \frac{(1-\eta) |U_p/U_0| \{ 2\eta^2 \ln \eta + (1-\eta^2) \} / \eta \ln \eta}{\{ 1 - [(\eta^2 - 1)/\ln \eta^2] + [(\eta^2 - 1)/\ln \eta^2] \ln [(\eta^2 - 1)/\ln \eta^2] \} \{ (1-\eta)^2 \lambda(1, \eta) + \alpha^2 + (1-\eta)^2 (n-1)^2 \}},$$

$$a_3 = \frac{|U_c/U_0|}{\{ \ln \eta(1-\eta) \lambda(-1, \eta) + \eta \alpha^2 + (1-\eta)^2 (n-1)^2 \}},$$

$$a_4 = \frac{1}{1-\eta} \left\{ \frac{1}{2} \left( \frac{\pi^2}{(\ln \eta)^2} + 1 \right) \right\}^{-\frac{1}{2}} a_1,$$

$$a_5 = (1/\eta) \{ \frac{1}{2} (1-\eta)^2 [\lambda(1, \eta) + 1] \}^{-\frac{1}{2}} a_2,$$

and

$$a_6 = \{ \frac{1}{2} \eta (1-\eta)^2 [\lambda(-1, \eta) + 1] \}^{-\frac{1}{2}} a_3.$$

Proof of Lemma 3

In view of lemma 1, it will suffice to consider only positive  $n$ . The eigenvalues ( $\rho_E$ ) of (4.1) satisfy the following integral relation:

$$1/\rho_E = I_{\alpha n}/D_{\alpha n}, \tag{4.15}$$

where

$$I_{\alpha n} = -\text{Re} \langle rD(V/r) wv + DUwu \rangle, \tag{4.16}$$

and

$$D_{\alpha n} = \left\langle |Dw|^2 + |Dv|^2 + |Du|^2 + \alpha^2(|w|^2 + |v|^2 + |u|^2) + \frac{n^2}{r^2} |u|^2 + \frac{|nw + iv|^2}{r^2} + \frac{|nv - iw|^2}{r^2} \right\rangle. \tag{4.17}$$

Here 'Re' denotes the real part. To obtain (4.15), multiply the first, second, and third of equations (4.1) by  $w^*$ ,  $v^*$ , and  $u^*$ , respectively; integrate and then rearrange.

We need to estimate  $I_{\alpha n}$  from above and  $D_{\alpha n}$  from below. By the Schwarz and Cauchy inequalities, using the expressions (2.2), (2.4) for  $V$  and  $U$ , we have that

$$\operatorname{Re} \left\langle wvrD \left( \frac{V}{r} \right) \right\rangle \leq b_1 \left\{ \left\langle \frac{|v|^2}{r} \right\rangle \left\langle \frac{|w|^2}{r} \right\rangle \right\}^{\frac{1}{2}} \leq \frac{1}{2} b_1 \left\{ \left\langle \frac{|v|^2}{r} \right\rangle + \left\langle \frac{|w|^2}{r} \right\rangle \right\}, \tag{4.18}$$

and

$$\begin{aligned} \operatorname{Re} \langle wuD U \rangle &\leq b_2 \langle |u|^2 \rangle \langle |w|^2 \rangle^{\frac{1}{2}} + b_3 \left\langle \frac{|u|^2}{r} \right\rangle \left\langle \frac{|w|^2}{r} \right\rangle^{\frac{1}{2}} \\ &\leq \frac{1}{2} b_2 \{ \langle |u|^2 \rangle + \langle |w|^2 \rangle \} + \frac{1}{2} b_3 \left\{ \left\langle \frac{|u|^2}{r} \right\rangle + \left\langle \frac{|w|^2}{r} \right\rangle \right\}, \end{aligned} \tag{4.19}$$

where  $b_1 = \frac{2\eta |R_1(\Omega_2 - \Omega_1)/U_0|}{(1 + \eta)(1 - \eta)^2}$ ,

$$b_2 = \frac{|U_D/U_0| \{2\eta^2 \ln \eta + (1 - \eta^2)\} (1 - \eta)}{\eta \ln \{1 - [(\eta^2 - 1)/\ln \eta^2] + [(\eta^2 - 1)/\ln \eta^2] \ln [(\eta^2 - 1)/\ln \eta^2]\}},$$

and  $b_3 = \frac{|U_c/U_0|}{\ln \eta}$ .

One can also show that (4.16) is dominated by quantities proportional to the wave-number. For this purpose, we use the last of equations (4.1) ( $\operatorname{div} \mathbf{u} = 0$ ) and find that

$$\langle |Dw|^2 \rangle + \left\langle \frac{|w|^2}{r} \right\rangle = \left\langle \frac{nw}{r} + \alpha u \right\rangle \leq 2\alpha^2 \langle |u|^2 \rangle + 2n^2 \left\langle \frac{|v|^2}{r} \right\rangle.$$

Then, using (4.12), (4.13) for the terms on the left, we find that

$$\left. \begin{aligned} b_4 \left\langle \frac{|w|^2}{r} \right\rangle &\leq b_5 \alpha^2 \left\langle \frac{|u|^2}{r} \right\rangle + b_6 n^2 \left\langle \frac{|v|^2}{r} \right\rangle, \\ b_7 \left\langle \frac{|w|^2}{r} \right\rangle &\leq b_8 \alpha^2 \left\langle \frac{|u|^2}{r} \right\rangle + b_9 n^2 \left\langle \frac{|v|^2}{r} \right\rangle, \\ b_{10} \langle |w|^2 \rangle &\leq b_{11} \alpha^2 \langle |u|^2 \rangle + b_{12} n^2 \langle |v|^2 \rangle, \end{aligned} \right\} \tag{4.20}$$

where  $b_4 = \frac{1}{2} \left( \frac{\pi^2}{(\ln \eta)^2} + 1 \right)$ ,  $b_7 = \frac{1}{2} (1 - \eta) \{ \lambda(-1, \eta) + 1 \}$ ,  
 $b_{10} = \frac{1}{2} (1 - \eta)^2 \{ \lambda(1, \eta) - 1 \}$ ,  $b_5 = 1/(1 - \eta)^2$ ,  $b_6 = b_{11} = 1$ ,  
 $b_8 = (1 - \eta)^{-1}$ ,  $b_9 = (1 - \eta)/\eta$ ,  $b_{12} = [(1 - \eta)/\eta]^2$ .

Now, using the estimates (4.20) and the second of the estimates (4.18), (4.19), we find

$$\begin{aligned} \operatorname{Re} \left\langle wvrD \left( \frac{V}{r} \right) \right\rangle &\leq \frac{b_1}{(b_4)^{\frac{1}{2}}} \left\{ b_5 \alpha^2 \left\langle \frac{|v|^2}{r} \right\rangle \left\langle \frac{|u|^2}{r} \right\rangle + b_6 n^2 \left\langle \frac{|v|^2}{r} \right\rangle^2 \right\}^{\frac{1}{2}} \\ &\leq b_1 \left\{ \frac{b_5}{b_4} \alpha^2 + \frac{b_6}{b_4} n^2 \right\}^{\frac{1}{2}} \left\langle \frac{|u|^2}{r} \right\rangle, \end{aligned} \tag{4.21}$$

and

$$\begin{aligned} \operatorname{Re} \langle wuD v \rangle &\leq \frac{b_2}{(b_{10})^{\frac{1}{2}}} \{ b_{11} \alpha^2 \langle |u|^2 \rangle^2 + b_{12} n^2 \langle |u|^2 \rangle \langle |v|^2 \rangle \}^{\frac{1}{2}} \\ &\quad + \frac{b_3}{(b_7)^{\frac{1}{2}}} \left\{ b_8 \alpha^2 \left\langle \frac{|u|^2}{r} \right\rangle^2 + b_9 n^2 \left\langle \frac{|u|^2}{r} \right\rangle \left\langle \frac{|v|^2}{r} \right\rangle \right\}^{\frac{1}{2}} \\ &\leq b_2 \left\{ \frac{b_{11}}{b_{10}} \alpha^2 + \frac{b_{12}}{b_{10}} n^2 \right\}^{\frac{1}{2}} \langle |\mathbf{u}|^2 \rangle + b_3 \left\{ \frac{b_8}{b_7} \alpha^2 + \frac{b_9}{b_7} n^2 \right\}^{\frac{1}{2}} \left\langle \frac{|\mathbf{u}|^2}{r} \right\rangle. \end{aligned} \tag{4.22}$$

We next estimate  $D_{xn}$  from below:

$$\begin{aligned}
 D_{xn} &\geq \{(1-\eta)^2\lambda(0,\eta) + \alpha^2\} \langle |w|^2 + |v|^2 \rangle \\
 &\quad + \{(1-\eta)^2\lambda(0,\eta) + (1-\eta)^2n^2 + \alpha^2\} \langle |u|^2 \rangle \\
 &\quad + (1-\eta)^2 \langle |nw + iv|^2 + |nv - iw|^2 \rangle \\
 &\geq \{(1-\eta)^2\lambda(0,\eta) + \alpha^2 + (1-\eta)^2(n^2 + 1)\} \langle |w|^2 + |v|^2 \rangle \\
 &\quad + \{(1-\eta)^2\lambda(0,\eta) + \alpha^2 + (1-\eta)^2n^2\} \langle |u|^2 \rangle \\
 &\quad - 2n|\langle w^*v \rangle - \langle v^*w \rangle| (1-\eta)^2 \\
 &\geq \{(1-\eta)^2\lambda(0,\eta) + \alpha^2 + (1-\eta)^2(n-1)^2\} \langle |\mathbf{u}|^2 \rangle = b_{13} \langle |\mathbf{u}|^2 \rangle. \tag{4.23}
 \end{aligned}$$

In a similar way, we find

$$D_{xn} \geq \left\{ \frac{\pi^2}{(\ln \eta)^2} + \frac{\alpha^2 \eta^2}{(1-\eta)^2} + (n-1)^2 \right\} \left\langle \frac{|\mathbf{u}|^2}{r} \right\rangle \equiv b_{14} \left\langle \frac{|\mathbf{u}|^2}{r} \right\rangle, \tag{4.24}$$

and

$$D_{xn} \geq \left\{ (1-\eta)\lambda(-1,\eta) + \frac{\eta\alpha^2}{1-\eta} + (1-\eta)(n-1)^2 \right\} \left\langle \frac{|\mathbf{u}|^2}{r} \right\rangle \equiv b_{15} \left\langle \frac{|\mathbf{u}|^2}{r} \right\rangle. \tag{4.25}$$

We form the ratio  $I_{xn}/D_{xn}$  and estimate  $I_{xn}$  with the last inequality of (4.18) and (4.19) and  $D_{xn}$  with (4.23), (4.24), (4.25) to find that

$$\frac{1}{\rho_E} \leq \frac{1}{2} \left( \frac{b_1}{b_{14}} + \frac{b_2}{b_{13}} + \frac{b_3}{b_{15}} \right) \equiv \frac{1}{2}(a_1 + a_2 + a_3).$$

Next, we estimate  $I_{xn}$  with (4.21), (4.22) and  $D_{xn}$ , as before, to find

$$\frac{1}{\rho_E} \leq a_1 \left\{ \frac{b_5}{b_4} \alpha^2 + \frac{b_6}{b_4} n^2 \right\}^{\frac{1}{2}} + a_2 \left\{ \frac{b_{11}}{b_{10}} \alpha^2 + \frac{b_{12}}{b_{10}} n^2 \right\}^{\frac{1}{2}} + a_3 \left\{ \frac{b_8}{b_7} \alpha^2 + \frac{b_9}{b_7} n^2 \right\}^{\frac{1}{2}}.$$

This proves lemma 3.

The estimate of the lemma shows that  $1/\rho_E \rightarrow 0$  as  $\alpha^2 + (1-\eta)^2n^2$  tends to zero or infinity. It follows that  $1/\rho_E$  takes on its maximum for a finite value of  $\alpha^2 + (1-\eta)^2n^2$ . Moreover, the lemma gives an explicit and rigorous bound on this maximum value. For example, for Couette flow between rotating cylinders ( $U_c^2 + U_p^2 = 0$ ), one finds that

$$\begin{aligned}
 \frac{1}{\rho_E} &\leq \left[ \frac{2\eta/(1+\eta)}{[\pi^2(1-\eta)^2/(\ln \eta)^2] + \alpha^2\eta^2 + (1-\eta)^2(n-1)^2} \right] \\
 &\quad \times \min \left\{ \frac{1}{2}, \frac{1}{2(1-\eta)} \left[ \frac{\pi^2}{2(\ln \eta)^2} + \frac{1}{2} \right]^{-\frac{1}{2}} (\alpha^2 + (1-\eta)^2n^2)^{\frac{1}{2}} \right\}. \tag{4.26}
 \end{aligned}$$

This estimate is a slight improvement of the estimate

$$\frac{1}{\rho_E} \leq \frac{\eta/(1+\eta)}{\pi^2(1-\eta)^2/(\ln \eta)^2}, \tag{4.27}$$

which has been given by Serrin (1959). Serrin's estimate ( $\rho < 10.92$  for Taylor's apparatus,  $\eta = 0.88$ ) is about  $\frac{1}{4}$  of the value given by the actual solution of the maximum problem ( $\rho < 44.5$ ). This gives a rough estimate of the numerical accuracy of the estimates of lemma 3.

It should be noted that with certain obvious changes in the definition of the constants  $b_i$ , one could use these estimates for any fields  $U(r)$  and  $V(r)$  and not just the ones mentioned in §2. The estimates are explicit in dependence on domain parameters  $(\alpha, n, \eta)$  and are uniformly bounded on any closed interval  $\eta_0 \leq \eta \leq 1$ ,  $\eta_0 > 0$ . In the limit  $\eta \rightarrow 1$ ,  $(1 - \eta)^2(n - 1)^2 \rightarrow n^2(1 - \eta)^2 \rightarrow \beta^2$ . There can be no differential rotation when  $\eta \rightarrow 0$ . Then we have Hagen–Poiseuille flow, which was treated separately by Joseph & Carmi (1969).

**5. Linear (instability) eigenvalue problem**

The estimates of lemmas 2 and 3 hold, also, for the linear problem. To see this, set  $\mathbf{u} \cdot \nabla \mathbf{u} = 0$  in (3.1), then use normal modes proportional to  $\exp\{i(\alpha x + n\phi) + \omega t\}$  where  $\omega$  is complex. In this way, we arrive at the equations

$$\left. \begin{aligned} \text{Re}(\omega) + i\mathcal{S}w - 2\frac{\tilde{V}}{r}v &= -Dp + \frac{1}{\rho} \left[ \mathcal{L}_n w - \frac{2in}{r^2}v \right], \\ \text{Re}(\omega) + \frac{w}{r}D(\tilde{V}r) + i\mathcal{S}v &= -\frac{inp}{r} + \frac{1}{\rho} \left[ \mathcal{L}_n v + \frac{2in}{r^2}w \right], \\ \text{Re}(\omega) + i\mathcal{S}u + wDU &= -i\alpha p + \frac{1}{\rho}L_n u, \end{aligned} \right\} \tag{5.1}$$

$$\mathcal{S} = (n/r)\tilde{V} + \alpha U - \text{Im}(\omega),$$

where  $\tilde{V} = V + \Omega r$ , and  $u, v, w$  satisfy (4.2).

LEMMA 4. Let  $\rho = \rho_L(\mathcal{S}, U, \tilde{V}, \alpha, n) > 0$  be the largest number such that all eigenvalues  $\omega$  of (5.1) and (4.2) have  $\text{Re}(\omega) \leq 0$ . Then  $\rho_L^{-1}(\alpha, n) \leq \rho_E^{-1}(\alpha, n)$ , and the estimate (4.14) holds, also, for  $1/\rho_L$ . Let  $\text{Re}(\omega) = 0$ . Then there is symmetry for the disturbance† given by

$$\begin{aligned} \rho_L(\mathcal{S}, U, \tilde{V}, \alpha, n) &= \rho_L(\mathcal{S}, -U, \tilde{V}, -\alpha, n) = \rho_L(-\mathcal{S}, -U, \tilde{V}, \alpha, -n) \\ &= \rho_L(-\mathcal{S}, U, \tilde{V}, -\alpha, n) = \rho_L(\mathcal{S}, U, -V, \alpha, -n) \\ &= \rho_L(-\mathcal{S}, U, \tilde{V}, -\alpha, -n). \end{aligned} \tag{5.2}$$

The estimates of lemma 3 hold for  $\rho_L$ , because we can form energy integrals for  $\rho_L$  directly from (5.1), and the real part of these integrals gives

$$\rho_L^{-1} = I_{zn}/D_{zn} \leq \max(I_{zn}/D_{zn}) = \rho_E^{-1},$$

as before. The imaginary part of the integrals could be used for estimates of the growth rate (Joseph 1969; Carmi 1969).

The symmetry result is proved here as in the proof of (4.7). For example, corresponding to (1) of that proof, we show invariance when

$$(\mathcal{S}, U, \tilde{V}, \alpha, n) \rightarrow (\mathcal{S}, -U, \tilde{V}, -\alpha, n) \quad \text{and} \quad (u, v, w, p) \rightarrow (-u, v, w, p).$$

† Equations (5.2), like those of lemma 1, give the ‘screw’ for the disturbance. Here, in addition to the requirement that  $nV$  and  $\alpha U$  have the same sign, we need that this be the sign of the wave speed  $\text{Im} \omega$ .

### 6. Conditions for the non-existence of sublinear instability

The possibility that instability can be initiated by non-linear disturbances for sublinear values of the stability parameters can be eliminated when the energy and linear limit coincide. This limit is, then, both necessary and sufficient for stability. Our inquiry, here, is about the possibility of finding values of the parameters which bring the linear limit as close as possible to the energy limit. It is convenient to think of spiral Couette flow, and for this the parameters are, say,  $\Omega_2 - \Omega_1$ ,  $\Omega_2$ ,  $\eta$  and  $U_c$ .† The linear limit  $\nu_L(\Omega_2 - \Omega_1, \Omega_2, U_c, \eta)$  depends on these parameters, but the energy limit  $\nu_E(\Omega_2 - \Omega_1, U_c, \eta)$  depends on one less parameter. We will seek the values of  $\Omega_2$  which make the value  $\nu_L - \nu_E$  smallest.

We will want to compare the eigenvalue problems (E) and (L), which are defined below. In these problems, equations (3.2b, c) hold. The problem (E) is to find a vector  $\mathbf{u}$  satisfying the above conditions and an eigenvalue  $\omega(\nu)$  such that

$$\omega(\nu) \mathbf{u} + \mathbf{u} \cdot \mathcal{D} - \nu \Delta \mathbf{u} + \nabla p = 0. \tag{E}$$

Since  $\mathcal{D}$  is symmetric  $\omega$  is necessarily real. The energy eigenvalues  $\hat{\nu}$  of (3.6) correspond to a zero eigenvalue  $\omega(\hat{\nu}) = 0$  of (E), and  $\nu_E$  is the largest of the eigenvalues  $\hat{\nu}$  of (3.6). The perturbation formula

$$\dot{\omega} \equiv \left. \frac{d\omega}{d\nu} \right|_{\nu=\hat{\nu}} = - \frac{\langle |\nabla \mathbf{u}|^2 \rangle}{\langle |\mathbf{u}|^2 \rangle} \tag{6.1}$$

follows in the usual way from (E) through the requirement that the right side of the equation expressing the first derivative of (E),

$$\omega \dot{\mathbf{u}} + \dot{\mathbf{u}} \cdot \mathcal{D} - \nu \Delta \dot{\mathbf{u}} + \nabla \dot{p} = \dot{\omega} \mathbf{u} + \Delta \mathbf{u},$$

be orthogonal to solutions of (E).

We want to know when an eigensolution of the problem (E) with eigenvalue  $\omega(\nu)$  is also a solution of the problem

$$\omega \mathbf{u} + 2\mathbf{\Omega} \times \mathbf{u} + \mathbf{u} \cdot \nabla \mathbf{U} + \mathbf{U} \cdot \nabla \mathbf{u} - \nu \Delta \mathbf{u} + \nabla p = 0. \tag{L}$$

Equation (L) and the boundary and side conditions define the spectral problem of linear theory.

**THEOREM 1.** *Suppose that (1)  $\mathbf{u}$  is an eigensolution of (E) and  $\omega(\nu)$  is its eigenvalue and (2) a vector  $\mathbf{\Omega}$  exists such that when*

$$\text{curl} \{ (\mathbf{U} \cdot \nabla) \mathbf{u} + 2\mathbf{\Omega} \times \mathbf{u} \} - \frac{1}{2} \{ (\text{curl } \mathbf{U} \cdot \nabla) \mathbf{u} - (\mathbf{u} \cdot \nabla) \text{curl } \mathbf{U} \} = 0, \tag{6.2}$$

*then  $\mathbf{u}$  is an eigensolution of (L) with eigenvalue  $\omega(\nu)$ .*

*If (1) and (2) hold when  $\nu_E - \epsilon < \nu \leq \nu_E$  ( $\epsilon > 0$ ) then  $\mathbf{U}$  is globally stable when  $\nu > \nu_E$ , and  $\mathbf{U}$  is unstable when  $\nu < \nu_E$ .*

*Proof of Theorem 1*

Since  $\mathbf{u}$  and  $\mathbf{U}$  are solenoidal,

$$\text{curl} \{ \mathbf{u} \cdot (\nabla \mathbf{U} - \mathcal{D}) \} = -\frac{1}{2} \text{curl} (\mathbf{u} \times \text{curl } \mathbf{U}) = -\frac{1}{2} \{ (\text{curl } \mathbf{U} \cdot \nabla) - (\mathbf{u} \cdot \nabla) \text{curl } \mathbf{U} \}.$$

† In §6 and §7, we use dimensional variables.

Then, if (6.2) holds,†

$$(\mathbf{U} \cdot \nabla) \mathbf{u} + 2\boldsymbol{\Omega} \times \mathbf{u} + \mathbf{u} \cdot (\nabla \mathbf{U} - \mathcal{D}) = -\nabla \phi, \tag{6.3}$$

and we can write (*E*) as

$$\omega(\nu) \mathbf{u} + 2\boldsymbol{\Omega} \times \mathbf{u} + \mathbf{u} \cdot \nabla \mathbf{U} + \mathbf{U} \cdot \nabla \mathbf{u} = -\nabla(p + \phi) + \nu \Delta \mathbf{u}. \tag{6.4}$$

Comparison of (6.4) and (*L*) proves that  $\mathbf{u}$  is an eigensolution of (*L*) with eigenvalue  $\omega(\nu)$ .

It has been shown (in §3) that if  $\nu > \nu_E$ , then the basic motion  $\mathbf{U}$  is globally stable. For instability, it suffices to have  $\omega(\nu) > 0$  in the spectral problem (*L*). Then, there will exist disturbances (solutions of (3.1)) which do not decay to zero (Yudovich 1965; Kirchgässner & Sorger 1968; Sattinger 1969). We have instability when  $\nu < \nu_E$  because then, by (6.1),  $\omega(\nu) > \omega(\nu_E) = 0$ . This completes the proof.

The theorem is not deep since so much of it is an assumption. But the formula (6.2) is important because it gives a computational procedure for finding the parameters of deepest instability when the assumptions hold, and for approximating these parameters when the assumptions hold approximately.

To apply (6.2), one needs only certain general properties of the energy eigenfunctions  $\mathbf{u}$ . For plane Couette flow ( $\mathbf{U} = \mathbf{e}_x \tilde{B}z$ ) in a rotating co-ordinate system  $\boldsymbol{\Omega} = \Omega_x \mathbf{e}_x + \Omega_y \mathbf{e}_y$ , the energy problem can be reduced to the Bénard problem for *X* independent rolls (the energy result is independent of  $\boldsymbol{\Omega}$ ). Then, (6.2) can be written as

$$\mathcal{U} \frac{\partial}{\partial \mathbf{X}} \text{curl } \mathbf{u} + \bar{D}U \frac{\partial}{\partial X} \begin{bmatrix} -v \\ u \\ 0 \end{bmatrix} - \left( 2\Omega_x \frac{\partial}{\partial X} + (\frac{1}{2}\tilde{B} + 2\Omega_y) \frac{\partial}{\partial Y} \right) \begin{bmatrix} u \\ v \\ w \end{bmatrix} = 0. \tag{6.5}$$

Equation (6.5) shows that the *X* independent energy eigenfunction solves the linear problem when

$$4\Omega_y = -\tilde{B}.$$

Or, one can satisfy (6.5) in the ‘fast rotation’ limit  $\alpha \rightarrow 0$ ,  $\Omega_x \rightarrow \infty$ ,  $\alpha\Omega_x = \text{const.}$  Since the ‘most unstable’ wave-number number for the Bénard problem is  $\beta = 3 \cdot 12 / (R_2 - R_1)$  (when  $\alpha = 0$ ), we have that

$$2\alpha\Omega_x - [3 \cdot 12 / (R_2 - R_1)] (\frac{1}{2}\tilde{B} + 2\Omega_y) = 0,$$

which gives the const. =  $\alpha\Omega_x$ .

The energy limit for Couette flow (Joseph 1966) is

$$\tilde{B}(R_2 - R_1) / \nu = 2\sqrt{1708}.$$

Theorem 1 guarantees that this limit is necessary and not only sufficient for the stability of two families of rotating Couette flows just described.

Busse (private communication) has given a different proof of the above result. It can also be obtained by comparison of the special linear solution of Kiessling (essentially that given in §9) with the energy result.

† For the doubly connected cylinder, one finds from (6.3) that since  $u = 0$ ,  $\partial\phi/\partial R = 0$  on the cylinders; this is sufficient to establish that  $\phi$  is single valued in the annulus.

There is, also, an exact 'fast rotation' result which holds for Poiseuille flow in a pipe. It can be obtained by comparison of Pedley's (1969) linear result with the energy result and leads to limit Reynolds numbers of about 100. This 'fast rotation' result holds, also, for rotating Couette-Poiseuille flow in the annulus (see § 11). †

To make further use of theorem 1, we need to develop the concept of an 'energy spiral' at a mean radius. We shall construct an argument, but not a proof, to support the guess that along the spiral, the energy eigenfunctions do not vary or vary slowly. The spiral idea allows us to draw the relevant information from the theorem directly, without solving eigenvalue problems. We shall verify our guess numerically for the important spiral Couette flow problem (figures 3, 4, § 8) which was investigated experimentally by Ludwig (1964). From now on, our analysis requires approximations, numerical work, or both.

## 7. The maximizing disturbance and the energy spiral

The disturbance  $\mathbf{u} \in \mathcal{h}$  which maximizes (3.4) we call the maximizing disturbance. For Couette flow [ $U_p = 0$ ] and Poiseuille flow [ $U_c = 0$ ] (when  $\eta > 0$ ), the maximizing disturbance is a longitudinal vortex with a streamwise axis. Such solutions do not vary in the direction of the stream. The same result is to be expected for every parallel flow for the following reason: One finds the energy limit as the solution of

$$\nu_E = \max_{\mathcal{h}} \{ -\langle uw dU/dZ \rangle / \langle |\nabla \mathbf{u}|^2 \rangle \}, \quad (7.1)$$

where  $\mathbf{U} = \mathbf{e}_x U(Z)$ ,  $u(X, Y, Z) = \mathbf{e}_x u + \mathbf{e}_y v + \mathbf{e}_z w = \mathbf{u} \left( X + \frac{2\pi}{\alpha}, Y + \frac{2\pi}{\beta}, Z \right)$ ,

$$\frac{\partial u}{\partial X} + \frac{\partial v}{\partial Y} + \frac{\partial w}{\partial Z} = 0, \quad (7.2)$$

and

$$u = v = w = 0|_{z=\pm \frac{1}{2}a}. \quad (7.3)$$

In general, we give to (7.1) its largest value when we can choose the product  $|wu|$  to have the largest possible value consistent with a positive value of  $-wu(dU/dZ)$  on each plane  $Z = \text{const.}$  while, at the same time, holding  $|\nabla \mathbf{u}|^2$  to the most moderate values compatible with (7.2) and (7.3). Very little can be done with the function  $w$ , since, by (7.3), it must vary (if it is not identically zero) between its zero value at the walls. But we could raise the value of  $wu$  by choosing larger  $u$  and, at the same time, hold the dissipation to small values and satisfy (7.2) among functions  $u, v, w$  which are independent of  $X$ , that is, among longitudinal vortices.

† It used to be thought that the linear limit for Poiseuille flow and Couette flow without rotation which ranges over Reynolds numbers ( $R$ ) in excess of 11,500, was in 'better agreement' with experiment than the  $O(100)$  numbers of energy theory. This incredible view (1) ignores the actual outcome of experiments and (2) misinterprets the meaning of the energy and linear criteria. The two theories are in splendid agreement with experiment: instability is always observed when  $R > R_L$  and stability prevails if  $R < R_B$ . For the interval  $R_L > R > R_B$  there exist stable disturbances whose energy initially increases and also sublinear instability. It is striking how rotation can reduce this interval where increasing stable disturbances and/or sublinear instabilities are possible.

A similar argument holds for the general spiral flow  $\mathbf{U} = \mathbf{e}_X U_X(R) + \mathbf{e}_\phi U_\phi(R)$ . Here, the maximum problem takes the form ( $\bar{D} = d/dR$ )

$$\nu_E = \max_{\bar{d}} \{ - \langle w(vR\bar{D}(U_\phi/R) + u\bar{D}U_X) \rangle / \langle |\nabla \mathbf{u}|^2 \rangle \}, \quad (7.4)$$

where  $\mathbf{e}_X u + \mathbf{e}_\phi v + \mathbf{e}_R w$  is single valued,

$$\mathbf{u}(R, \phi, X) = \mathbf{u}(R, \phi, X + 2\pi/\alpha), \quad \frac{1}{R} \frac{\partial}{\partial R} (wR) + \frac{1}{R} \frac{\partial v}{\partial \phi} + \frac{\partial u}{\partial X} = 0, \quad (7.5)$$

and

$$\bar{u} = \bar{v} = \bar{w} = 0 \Big|_{R=R_1, R_2}. \quad (7.6)$$

As in the earlier argument, we expect the maximizing function for (7.4) to be found among the functions which allow one to raise the value of

$$-w(vR\bar{D}(U_\phi/R) + u\bar{D}U_X)$$

without too sharply increasing the value of the dissipation denominator of (7.4). The function  $w$ , as before, is not suited for this purpose, but one can raise the value of  $-(vR\bar{D}(U_\phi/R) + u\bar{D}U_X)$  without increasing the dissipation too sharply among functions  $w$ ,  $u$  and  $v$ , which do not vary (or vary slowly) in the direction of the disturbance-velocity component

$$u' \sim vR\bar{D}(U_\phi/R) + u\bar{D}U_X. \quad (7.7)$$

It will be useful to give a bit more structure to this idea about the nature of the maximizing functions. Consider a tangent plane to the cylinder at

$$R = \frac{1}{2}(R_1 + R_2).$$

Let  $\mathbf{e}_x$  and  $\mathbf{e}_y$  be unit vectors in the direction of  $u'$  and  $v'$ , respectively, and  $\mathbf{e}_x \cdot \mathbf{e}_x = \cos \psi$  (figure 2). The direction  $X'$  of the maximizing disturbance  $u'$ ,  $w$ ,  $v' (= 0)$  is to be expected to have the direction given by the angle  $\psi$ , where

$$\tan \psi = \left. \frac{R\bar{D}(U_\phi/R)}{\bar{D}U_X} \right|_{R=\frac{1}{2}(R_1+R_2)}. \quad (7.8)$$

In this direction, the maximizing function should not vary, or should vary slowly,

$$0 \approx \frac{\partial}{\partial X'} = \cos \psi \frac{\partial}{\partial X} + \frac{2 \sin \psi}{R_1 + R_2} \frac{\partial}{\partial \phi}, \quad (7.9)$$

which, for normal modes proportional to  $\exp\{i(\bar{\alpha}X + n\phi)\}$ , gives the spiral angle

$$\tan \psi = \frac{-\bar{\alpha}}{2n} (R_1 + R_2). \quad (7.10)$$

As we shall see, this argument holds nearly for all  $\eta$  not too hopelessly small, and exactly for  $\eta \rightarrow 1$  when  $U_x(R)$  is of the form (2.3) or (2.2) with  $U_p = 0$ .

We want, next, to draw the consequences of theorem 1 for the general spiral flow. In polar cylindrical co-ordinates  $(R, \phi, X)$ , we can write (6.2) as

$$0 = \text{curl} \left\{ e_i \left( U_X \frac{\partial u_i}{\partial X} + \frac{U_\phi}{R} \frac{\partial u_i}{\partial \phi} \right) \right\} + e_i \left\{ \frac{1}{2R} \bar{D}U_X \frac{\partial u_i}{\partial \phi} - \left[ 2\Omega + \frac{U_\phi}{R} + \frac{1}{2R} \bar{D}(RU_\phi) \right] \frac{\partial u_i}{\partial X} \right\} \\ + \frac{1}{2} \mathbf{e}_\phi w R \bar{D} \left( \frac{1}{R} \bar{D}U_X \right) + \mathbf{e}_X w \bar{D} \left( \frac{U_\phi}{R} \right), \quad (7.11)$$



where

$$e_i u_i = e_x u + e_\phi v + e_r w$$

is a solution (normalized with  $\langle |\mathbf{u}|^2 \rangle = 1$ ) of the energy problem, and we have put  $\bar{D}((1/R)\bar{D}(RU_\phi)) = 0$  in accord with (2.1). Equation (7.11) can be satisfied exactly only in the limit ( $R_2 - R_1 = d$ ,  $R_1 \rightarrow \infty$ ,  $\eta \rightarrow 1$ ). Otherwise, if it holds at one value of  $R$ , it cannot hold at another value of  $R$ . But in §8, we will show that it is a good approximate result which gives the values of the parameters corresponding to the deepest instability where the energy and linear limits are closest.

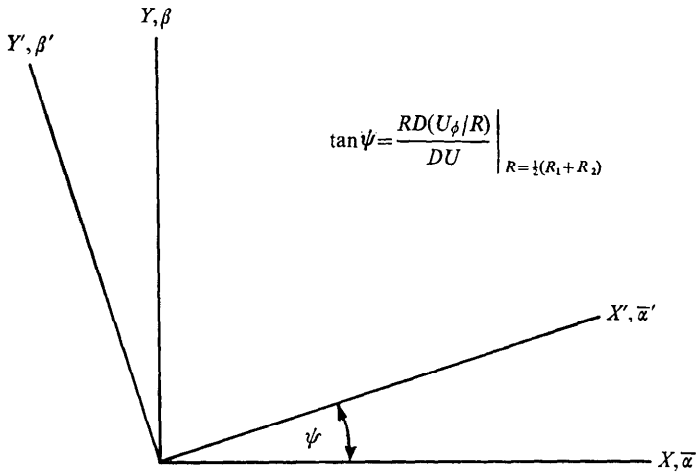


FIGURE 2. Energy spiral. Along  $X'$  the energy disturbance does not vary or varies slowly. There is a value of  $R_1 \leq R_0 \leq R_2$  such that the energy spiral at the mean radius coincides with the basic stream spiral at  $R_0$  for an observer rotating with angular velocity  $\Omega = \Omega_2$ . (For justification, see figure 5.) To such an observer, the basic flow appears as a combination of axial and circumferential shears. That is, the basic flow velocity is zero, to such an observer, at the outer cylinder. For certain parameter values, the angle  $\psi$  is also the angle between  $X$  and the spiral axis of the linear disturbance vortex.

To use it, first put  $R = \frac{1}{2}(R_1 + R_2)$ ; second, at this  $R$ , consider disturbances of the energy type (7.9) for which  $\partial/\partial X + \tan \psi (\partial/R\partial\phi) = 0$ , and find the value of  $\Omega$  which makes the derivative  $\mathbf{U} \cdot \nabla$  in the direction of the basic flow a derivative in the direction of the energy spiral. Then, in the first bracket of (7.11), we may set

$$0 = (\mathbf{U} \cdot \nabla) u_i = \{-U_X \tan \psi + U_\phi\} \frac{1}{R} \frac{\partial u_i}{\partial \phi}, \tag{7.12}$$

where  $U_X$  (2.2) and  $\psi(R)$  (7.8) are evaluated at  $R = \frac{1}{2}(R_1 + R_2)$ , and then select  $\Omega_2$  to make the second bracket of (7.11) vanish

$$\frac{1}{2} \bar{D} U_X \cot \psi + 2\Omega + U_\phi/R + (1/2R) \bar{D}(RU_\phi) = 0, \tag{7.13}$$

where  $\partial/\partial X$  has been eliminated with (7.9).

Given that (7.12) and (7.13) must satisfy (7.11) at the mean radius, we have

$$0 = \frac{1}{2} e_\phi (\bar{D}^2 U_X - (1/R) \bar{D} U_X) w + e_X \bar{D}(U_\phi/R) w. \tag{7.14}$$

It is possible to satisfy (7.14) exactly when  $U_p = 0$  and  $\eta \rightarrow 1$  or when  $U_\phi = 0$  and  $U_X$  has the form (2.3). Consider the case  $U_p = 0$ . Then, at  $R = \frac{1}{2}(R_1 + R_2)$ , (7.14) can be written as

$$\left\{ \mathbf{e}_\phi \frac{U_c(1-\eta)^2}{(1+\eta)^2 \ln \eta} + \mathbf{e}_x \frac{R(\Omega_2 - \Omega_1) 16\eta(1-\eta)}{(1+\eta)^4} \right\} w = 0. \quad (7.15)$$

This can be satisfied identically not only when  $\eta \rightarrow 1$ , but also when  $\eta \rightarrow 0$ . The value of  $w$ , itself, may be expected to be small relative to  $\langle |\mathbf{u}|^2 \rangle$  in that both  $w = 0$  and  $\bar{D}w = 0$  hold at the boundaries. For parabolic flow of type (2.3), the coefficient of  $\mathbf{e}_\phi$  vanishes identically at all  $R_1 \leq R \leq R_2$ . It follows that for spiral Couette flow and spiral parabolic flow, it may be possible to make the distance between the energy and linear limits very small by choosing the parameters  $\Omega$  and  $\Omega_2$  to reduce (7.12), (7.13) to an identity. The considerable extent to which this possibility is realized is revealed in § 8 for the Couette flow and in § 11 for the parabolic flow.

## 8. Spiral Couette flow

We set  $U_p = 0$  and use (7.8) to write (7.12) at the mean radius as

$$A' = -\frac{B}{R^2} \left\{ \frac{2U_\phi}{R\bar{D}U_X} + 1 \right\} = -\frac{4B}{R_2^2(1+\eta)^2} \{ 2 \ln \frac{1}{2}(1+\eta) + 1 \}, \quad A' = A - \Omega, \quad (8.1)$$

where  $A$  and  $B$  are given by (2.1). Equation (7.13) may, then, be written as

$$2\Omega + 2A' + \frac{B}{R^2} - \frac{U_c^2}{4(\ln \eta)^2 B} = 2\Omega + 2A' + \frac{4B}{R_2^2(1+\eta)^2} - \frac{U_c^2}{4B(\ln \eta)^2}. \quad (8.2)$$

The angular velocity of the observer for whom the disturbance giving the deepest instability is steady is obtained from (8.1) as

$$\Omega = \Omega_2 - \gamma(\eta) (\Omega_1 - \Omega_2), \quad \left. \begin{aligned} \text{where} \\ \gamma(\eta) = \frac{\eta^2}{(1-\eta^2)} \left\{ 1 - \frac{4(1-2 \ln \frac{1}{2}(1+\eta))}{(1+\eta)^2} \right\} \end{aligned} \right\} \quad (8.3)$$

We note that  $\gamma > 0$  for  $0 < \eta < 1$ , and  $\gamma(0) = \gamma(1) = 0$ . Also,  $\gamma(\eta)$  has a relatively small maximum of about 0.082 occurring at  $\eta \approx 0.49$ . Hence, in the two limiting cases of  $\eta = 1$ ,  $\eta = 0$ , such disturbances appear steady to an observer rotating with the outer cylinder, while for other  $\eta$ , the angular velocity of the observer is given by (8.3). This expression is valid for a choice of parameters for which the instability limit is as close as possible to the stability limit, that is, in the set of parameters for which (6.2) holds. This set is determined from (8.2), which can be written as

$$\frac{(1-\eta)}{(1+\eta)} \frac{\Omega_2}{(\Omega_2 - \Omega_1)} + \frac{2\eta^2}{(1+\eta)^4} \left( \frac{1}{2}\eta^2 + \eta - \frac{1}{2} \right) + \left( \frac{U_c}{R_1(\Omega_1 - \Omega_2)} \right)^2 \frac{1}{8} \left( \frac{1-\eta}{(1+\eta) \ln \eta} \right)^2 = 0. \quad (8.4)$$

On the other hand, the flow is unstable when

$$\frac{(R_2 - R_1) U_0}{\nu} > \rho_L(\chi, \Omega_2, \eta),$$

where  $\rho_L$  is the smallest positive value for which a solution (5.1) and (4.2) exists. When  $\eta = 1$ ,  $\rho_E = \rho_L$  and sublinear solutions are excluded for certain parameter values.

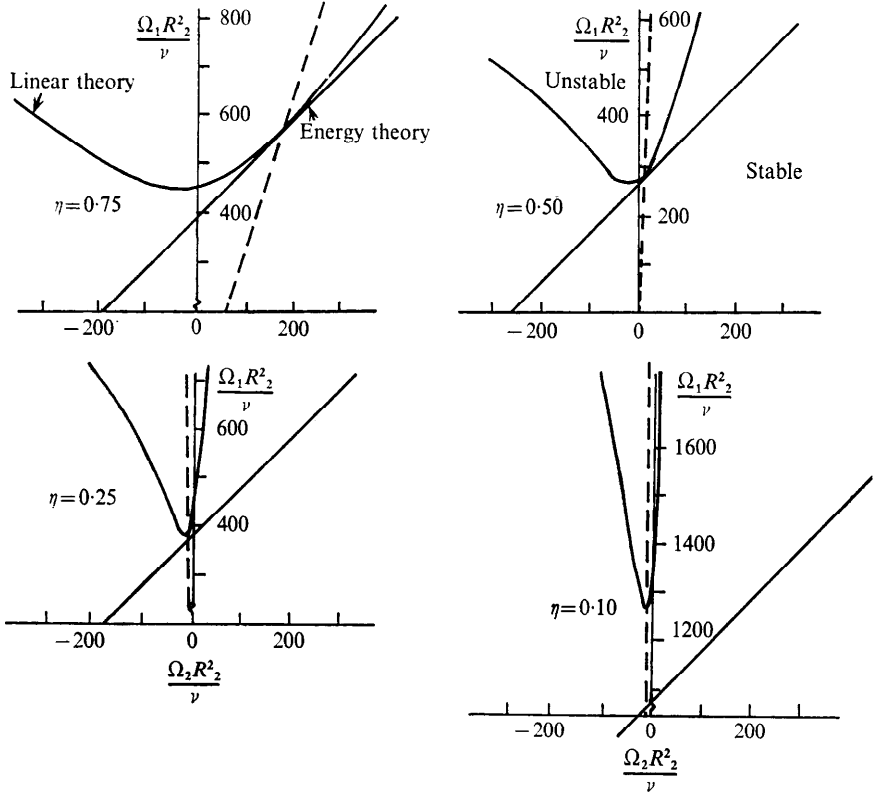


FIGURE 6. Energy and linear (Sparrow, Munro & Jonsson) results for Taylor flow as a function of radius ratio,  $\eta$ . The dashed line is a ray from the origin given by (8.6). Along the ray, the distance between the energy and linear limits is seen to be very nearly minimum.

To what extent is it possible to choose  $\Omega_2$  to make  $\rho_L - \rho_E$  small for  $\eta \neq 1$ ? We can answer this question for cylindrical Couette flow, because when  $U_c = 0$ , the linear limit is known from numerical calculations of Sparrow, Munro & Jonsson (1964). For  $U_c = 0$ , we know from numerical calculation that the energy limit is taken on for axisymmetric disturbances. Then, with

$$(\mathbf{U} \cdot \nabla) u_i = (U_\phi/R) \partial u_i / \partial \phi \equiv 0,$$

(7.12) holds identically and (8.1), (8.3) are lost. With  $U_c = 0$ , one has (8.4) in the form

$$\frac{\Omega_1}{\Omega_2} = \frac{1 + 2\eta - \eta^2}{\eta^2(\eta^2 + 2\eta - 1)}. \tag{8.6}$$

This is a ray from the origin in the  $\Omega_1, \Omega_2$  plane (figure 6). A unique point of the plane is determined by the intersection of this ray with the upper energy boundary. This is the point which should be closest to the linear limit. The ray (8.6) does follow this deepest instability quite exactly (figure 6); when  $\eta = 1$ , the ray (8.6) gives  $\Omega_1 = \Omega_2$  and coincides with the Rayleigh–Synge line. The point of closest approach moves down the energy border as  $\eta$  is decreased, passes through  $\Omega_2 = 0$  when  $\eta \approx 0.41$ , reaches a small, negative minimum when  $\eta \approx 0.26$ , and returns to  $\Omega_2 = 0$  as  $\eta \rightarrow 0$ .

We cannot test the accuracy of the criterion (8.4) when  $U_c \neq 0$ , because we have not calculated the linear limit for this case. But the assumption of a mean radius, which is central in the derivation of (8.4), gives a good approximation for the energy spiral  $\psi$  and the basic flow  $U_x, U_\phi$  in (7.12) and (7.13). We think (8.4) is an accurate criterion of about the same precision as its special ( $U_c = 0$ ) value (8.6).

## 9. The narrow-gap plus mean-radius approximation for spiral Couette flow.

The aim of the calculation of this section is a simple explicit theory to explain (1) Ludwig's ( $\eta = 0.8$ ) experiment and (2) future experiments to test the  $\eta$  variation.

The use of a mean radius already suggests an approximation to obtain the explicit stability limits. The approximation consists of replacing variable coefficients with constant coefficients at the mean radius and of making a narrow-gap approximation for the differential operators. † The approximation of the operators loses accuracy for small  $\eta$  but is exact in the limit  $\eta \rightarrow 1$ .

There is a distinction to be made between a mean radius approximation, like that which leads to (8.4), and the narrow-gap plus mean-radius approximation of this section. One has hope for the former when the coefficients are not too rapidly varying and do not change sign in the annulus. For example, (8.6) is a good criterion when  $\eta = 0.1$ , and it gives  $\Omega_2/\Omega_1 < 0$ , which contrasts sharply with the restrictions  $\Omega_2/\Omega_1 > 0$ ,  $1 - \eta$  small, set on the narrow-gap plus mean-radius approximation by Chandrasekhar.

The approximations are carried out as follows:

Consider the limit  $\eta \rightarrow 1$ ,  $\eta/(1 - \eta) \leq r \leq 1/(1 - \eta) \rightarrow \infty$  and  $n/r \rightarrow \beta$ . We have

$$\mathcal{L}_n w - \frac{2in}{r^2} v - Dp \rightarrow \mathcal{L}w - Dp, \quad \mathcal{L}_n v + \frac{2in}{r^2} w - \frac{inp}{r} \rightarrow \mathcal{L}v - i\beta p, \quad (9.1)$$

and

$$L_n u - i\alpha p \rightarrow \mathcal{L}u - i\alpha p,$$

where

$$\mathcal{L} \equiv D^2 - (\alpha^2 + \beta^2).$$

Equation (9.1) allows us to simplify the right-hand side of the energy equations

† Identical approximations are used by Chandrasekhar (1961, p. 309 and p. 375) to treat Couette flow between cylinders and combined Couette and Poiseuille (spiral) flow. Serrin (1968) shows how this approximation implies that the Taylor instability boundary is a hyperbola in the first and third quadrant of the  $\Omega_2, \Omega_1$  plane.

(4.1) and linear equations (5.1). We simplify the left-hand side by the mean-radius approximation and find that with

$$f(\chi, \eta) = \frac{8\eta}{(1+\eta)^3} \left[ \frac{\tan^2 \chi + g^2(\eta)}{\tan^2 \chi + 1} \right]^{\frac{1}{2}}, \quad g(\eta) = \frac{(1-\eta)(1+\eta)^2}{4\eta \ln \eta},$$

$$\sin \psi = \frac{8\eta \sin \chi}{(1+\eta)^3 f(\chi, \eta)}, \quad \cos \psi = -\frac{2(1-\eta) \cos \chi}{(1+\eta) f(\chi, \eta) \ln \eta}, \quad (9.2)$$

where  $\psi$  is the spiral angle (figure 2) and the angle  $\chi$  is defined by (8.5), the energy equation (4.1) can be written as

$$\left. \begin{aligned} -\frac{1}{2} \rho'_E f(\chi, \eta) \{v \sin \psi + u \cos \psi\} &= -Dp + \mathcal{L}w, \\ -\frac{1}{2} \rho'_E f(\chi, \eta) w \sin \psi &= -i\beta p + \mathcal{L}v, \\ -\frac{1}{2} \rho'_E f(\chi, \eta) w \cos \psi &= -i\alpha p + \mathcal{L}u, \end{aligned} \right\} \quad (9.3)$$

and the linear equations (5.1) as

$$\left. \begin{aligned} i\mathcal{S}w - \rho'_L f(\chi, \eta) \{2\Omega_\eta + \frac{1}{4}(1-\eta)(\eta+3) \sin \psi\} v &= -Dp + \mathcal{L}w, \\ \rho'_L f(\chi, \eta) \{2\Omega_\eta - \frac{1}{4}(1+\eta)^2 \sin \psi\} w + i\mathcal{S}v &= -i\beta p + \mathcal{L}v, \\ i\mathcal{S}u - \rho'_L f(\chi, \eta) \cos \psi w &= -i\alpha p + \mathcal{L}u, \end{aligned} \right\} \quad (9.4)$$

where

$$\Omega_\eta = \frac{1}{f(\chi, \eta)} \tilde{\Omega}_2, \quad \tilde{\Omega}_2 = \frac{\Omega_2(R_2 - R_1)}{[R_1^2(\Omega_1 - \Omega_2)^2 + U_c^2]^{\frac{1}{2}}}.$$

The primes indicate that the eigenvalues are associated with the mean-radius, narrow-gap solution. The continuity equation has the form

$$\left. \begin{aligned} Dw + i\alpha u + i\beta v &= 0, \\ u = v = w = 0 &|_{r=\eta/(1-\eta), 1/(1-\eta)}. \end{aligned} \right\} \quad (9.5)$$

Stability is guaranteed when  $(R_2 - R_1) [U_c^2 + R_1^2(\Omega_2 - \Omega_1)^2]^{\frac{1}{2}}/v < \min \rho_E$  and instability when  $> \rho_L$ . The eigenvalues  $\rho'_L$  and  $\rho'_E$  approach  $\rho_L$  and  $\rho_E$  as  $\eta \rightarrow 1$ , and approximate  $\rho_L$  and  $\rho_E$  for  $\eta$  near one (figure 4).

The most relevant wave-numbers for the deepest instabilities are not  $\alpha$  and  $\beta$ , but are the wave-numbers along the energy spiral, that is,  $\alpha'$  and  $\beta'$  (see figure 2). Using the wave-numbers, the energy system (9.3) can be reduced, in the usual way, to a single sixth-order equation,

$$\{\mathcal{L}^3 - i(\rho'_E f) \alpha' D\mathcal{L} + (\frac{1}{2} \rho'_E f)^2 \beta'^2\} w = 0, \quad (9.6)$$

with boundary conditions

$$w = Dw = \mathcal{L}^2 w = 0 \quad \text{at} \quad r = \eta/(1-\eta), \quad 1/(1-\eta). \quad (9.7)$$

The minimum eigenvalue  $(\rho'_E f)$  for (9.6), (9.7) is found for the disturbances  $\alpha' = 0$  which are transverse to the mean spiral flow and is given by

$$(\min \rho'_E) f(\chi, \eta) = 2(1708)^{\frac{1}{2}}, \quad \beta' = 3.12. \quad (9.8)$$

In figure 4, we have compared  $\rho'_E$  with the exact numerical result.

In the same way, we introduce  $\alpha'$  and  $\beta'$  into the linear equations (9.4) and then, by elimination of  $p$ ,  $u$  and  $v$  in that order, we obtain

$$\{\mathcal{L}(\mathcal{L} - i\mathcal{S})^2 - i\alpha'(\rho'_L f) D(\mathcal{L} - i\mathcal{S}) - (\rho'_L f)^2 F(\eta, \chi, \tilde{\Omega}_2)\} w = 0, \quad (9.9)$$

and  
Here,

$$w = Dw = \mathcal{L}(\mathcal{L} - i\mathcal{S})w = 0. \tag{9.10}$$

$$F(\eta, \chi, \tilde{\Omega}_2) = \left\{ \Omega_\eta + \frac{1}{8}(1 - \eta)(\eta + 3) \sin \psi \right\} \left\{ 4(\alpha' \cos \psi - \beta' \sin \psi)^2 \right. \\ \times \left( \Omega_\eta - \frac{1}{8}(1 + \eta)^2 \sin \psi \right) + 2(\alpha'^2 - \beta'^2) \sin \psi \cos^2 \psi + 2\alpha' \beta' \\ \left. \times (\cos^2 \psi - \sin^2 \psi) \cos \psi \right\}. \tag{9.11}$$

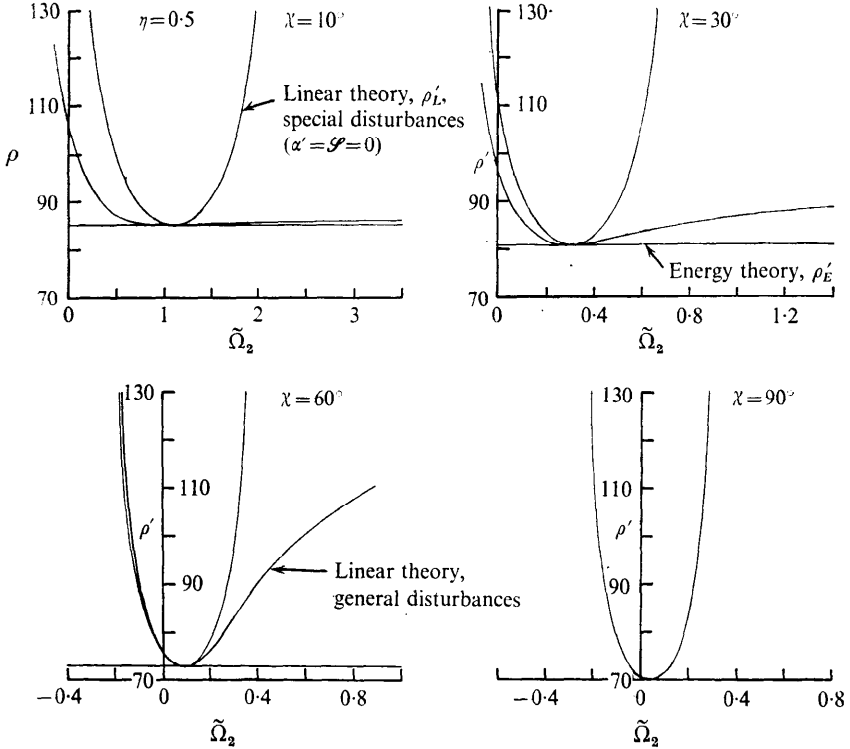


FIGURE 7. Comparison of approximate linear and energy results for disturbances in the direction of the energy spiral for  $0 < \chi \leq 90^\circ$  ( $0 < \Omega_1 < \Omega_2$ ) and  $\eta = 0.5$ . The top line is the eigenvalue belonging to a special linear solution whose spiral angle coincides with the energy spiral. The middle line is the smallest eigenvalue, and the spiral of its eigensolution does not, in general, correspond to the energy spiral. The bottom (horizontal) line is the energy eigenvalue. At the point of tangency, the linear and energy limits coincide, and sublinear instability can be excluded.

In general, we seek the minimum value of  $\rho'_L$  over  $\alpha', \beta'$ , and this must be found from the general solution of the problem. This solution can be expressed by the algebraic system which is equivalent to the differential equation [cf. Joseph 1966, p. 180]. As in a similar problem by Chandrasekhar (1961, p. 374), for given wave-numbers  $\alpha', \beta'$  and an arbitrary value of  $\mathcal{S}$ , the eigenvalue  $\rho'_L$  will, in general, be complex. Hence, we seek the value of  $\mathcal{S}$  which makes  $\rho'_L$  real. It can be shown (similar to Chandrasekhar 1961, p. 24) that if the eigenfunction  $w$  of (9.9) is symmetric with respect to the annulus centre, then  $\mathcal{S} = 0$ . The numerical calculation gave  $\mathcal{S} = 0$  in all cases.

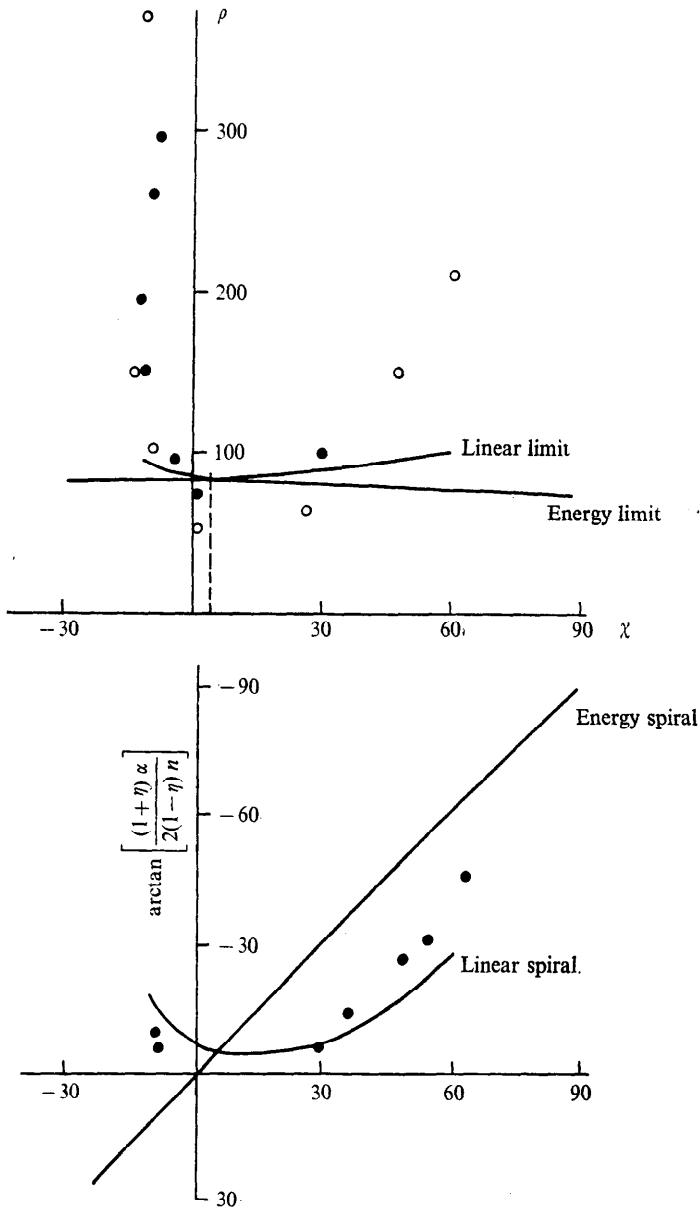


FIGURE 8. Comparison of Ludwig's (1964) experimental results with viscous linear theory and energy theory. For the experiment  $\eta = 0.8$ ,  $\Omega_2(R_2 - R_1)/\nu = 150$ . The dashed vertical line locates the value  $\chi$  for which the energy and linear results should, theoretically, come together. In (a), we have given the stability and instability limit, and in (b), the value of the spiral angle. Black dots are unstable, and white ones are stable.

For the energy spiral disturbances, an easier result is available. Consider (9.9) and (9.10) for  $\alpha' = \mathcal{S} = 0$ . This has the following meaning: From (5.1), it is possible to show that the energy spiral disturbances  $\alpha' = 0$ , when coupled with  $\mathcal{S} = 0$ , appear as steady disturbances as seen by an observer rotating with angular velocity  $\Omega$  given by (8.3). In the present context, this relationship (resulting from  $\alpha' = \mathcal{S} = 0$ ) is valid for any set of parameters of the basic flow, not just those in the set for which the instability and stability limits are closest, as discussed in §8. The resulting problem, again, is the Bénard problem, with the result

$$\rho'_{L'} f^2 = \frac{1708}{[2\Omega_\eta \sin \psi' + \frac{1}{4}(1-\eta)(3+\eta)\sin^2 \psi'] [\cos^2 \psi' + \frac{1}{4}(1+\eta)^2 \sin^2 \psi' - 2\Omega_\eta \sin \psi']}, \quad (9.12)$$

and

$$\beta' = 3.12. \quad (9.13)$$

Given the validity of the mean-radius, narrow-gap approximation, (9.12) is still a special case, and more general solutions (say,  $\alpha' \neq 0$ ,  $\mathcal{S} = 0$ ) can (do) give smaller values for  $\rho'_{L'}$ . Numerical calculations (Munson 1970) show that  $\mathcal{S} = 0$ ,  $\alpha' \neq 0$  gives to  $\rho'_{L'}$  its smallest value over the range of values ( $\chi$ ,  $\tilde{\Omega}_2$ ) considered in figures 7 and 8. However, it is easy to verify by comparing (9.12) and (9.8) that if we choose

$$\Omega_\eta = \frac{1}{4 \sin \psi'} [\cos^2 \psi' + \frac{1}{2}(\eta^2 + 2\eta - 1)\sin^2 \psi'], \quad (9.14)$$

then the  $\rho'_{L'}$  of (9.12) coincides with  $\min \rho'_{E'}$ . It is no surprise that (9.14) is exactly the criterion (8.4) which we derived without a narrow-gap approximation. The result  $\min \rho'_{E'} = \min \rho'_{L'}$ , which is obvious for the exact (unprimed,  $\eta = 1$ ) eigenvalues, is also true for the primed eigenvalues (figure 7).

## 10. Ludwig's experiments

We want now to compare our theoretical results with the experiments of Ludwig (1964). Ludwig's apparatus is like a long sleeve bearing which is rotated around its axis at a fixed angular velocity and is geared to a shaft in the bearing in such a way that the shaft can be made to turn and slide relative to the rotating bearing. Since the clearance is small ( $\eta = 0.8$ ), the flow develops almost instantly and is very nearly pure linear shear.

For  $\eta = 0.8$ , we find from (9.8) that

$$\rho'_{E'} = 75.3 \left[ \frac{\tan^2 \chi + 1}{\tan^2 \chi + 0.822} \right]^{\frac{1}{2}}.$$

The special solution (9.12) gives

$$\rho'_{L'} = \left\{ \frac{427[(\tan^2 \chi + 0.822)/(\tan^2 \chi + 1)]}{[\tilde{\Omega}_2 \sin \chi + 0.1045 \sin^2 \chi][0.45(\cos^2 \chi + 0.992 \sin^2 \chi) - \tilde{\Omega}_2 \sin \chi]} \right\}^{\frac{1}{2}},$$

and sublinear solutions can be excluded (in the approximation) along the curve  $\rho'_{E'}(\chi(\tilde{\Omega}_2), \tilde{\Omega}_2)$ , where  $\chi(\tilde{\Omega}_2)$  is the curve

$$\tilde{\Omega}_2 = \frac{0.225}{\sin \chi} [\cos^2 \chi + 0.757 \sin^2 \chi].$$



The graphs of  $\rho'_E$ ,  $\rho'_L$  and  $\chi(\tilde{\Omega}_2)$  are shown for a representative value of  $\eta$  ( $= 0.5$ ) in figure 7. The values of  $\rho'_E$  and  $\rho'_L$  differ by very little from the exact values  $\rho_E$  and  $\rho_L$  when  $\eta = 0.8$  (see figure 4), and we shall regard the primed values as the true limits in the discussion which follows.

In Ludwig's experiments, the parameter  $\Omega_2(R_2 - R_1)^2/\nu = 150$  is held fixed, and his results are expressed in terms of the parameters  $a$ ,  $\tilde{C}_z$  and  $\tilde{C}_\phi$ , which are related to the parameters of this paper as follows:

$$a = (1 - \eta)/(1 + \eta), \quad \rho = 150/\tilde{\Omega}_2,$$

$$\tilde{\Omega}_2 = (1 + a\tilde{C}_\phi)/\{(a + 1)^2\tilde{C}_z^2 + (1 - \tilde{C}_\phi)^2\}^{\frac{1}{2}},$$

and 
$$\chi = \arcsin \{(1 - \tilde{C}_\phi)/\{(a + 1)^2\tilde{C}_z^2 + (1 - \tilde{C}_\phi)^2\}^{\frac{1}{2}}\}.$$

Since Ludwig's data show considerable scatter, we have used a 'mean' value of  $\Omega_2$  to calculate the theoretical linear limit shown in figure 8 (cf. Munson 1970).

Ludwig's experiment shows that even without the centrifugal force mechanism for Taylor instability, the rigid rotation can provide a background in which disturbance Coriolis forces lower the threshold of instability from 2000 to near the energy value  $O(100)$ . Theoretically, at the values  $\tilde{\Omega}_2$ ,  $\chi(\tilde{\Omega}_2)$  for which the energy limit is attained (cf. figure 7), one can exclude the possibility of sublinear instability. This lowering of the threshold value for instability is a clear outcome of the experiment. So, too, the general spiral character of the observed instability supports the energy and linear analyses. The rather good agreement between the spiral angle and the linear theory does suggest that the observed mode can begin with an infinitesimal perturbation. It is worth noting that the observed spiral is in better accord with Ludwig's (1961) inviscid analysis than with the more complete viscous analysis given here.

For very fast solid rotation ( $\chi = 0$ ), both energy theory and linear theory indicate instability in vortices whose axes are nearly parallel to the cylinder axis, that is, the spiral is stretched out. Ludwig's (1964) data show this trend, and the photograph in the cited paper shows the elongated spiral quite clearly.

Unfortunately, the experiment cannot be said to answer one question posed by our comparison of energy and linear theory, that is, the possibility of instability for values of  $\rho$  between the energy and linear limits. This is true for two reasons. First, there is too much scatter in the data. One does not expect stable points (white dots) to lie above the instability (linear) limit or unstable points to lie below the stability (energy) limit. Secondly, and more important, even if the experiment and theory were a perfect match, one could not exclude the possibility that non-linear unstable modes exist by observing the existence of unstable linear modes.

There are four important observables in an experiment like Ludwig's: (1) the threshold limit, (2) the spiral angle, (3) the wave speed for the disturbances or the value of  $\Omega$  for which the deepest instability is steady (8.3), and (4) the spiral vortex spacing†. Only (1) and (2) are discussed by Ludwig.

† If every other white band in the photograph of Ludwig's paper is a cell, then the number of cells is that predicted by energy theory.

## 11. Poiseuille–Couette rotating flow

It is possible to reduce (7.11) to an identity for profiles of the parabolic form (2.3). For these profiles, one can also rule out sublinear instability. For a much wider class of flows where no exact result is available, we expect that (7.11) gives a good approximation to parameter values for which the motion is most unstable to small disturbances.

First, we consider parabolic profiles of the form (2.3) and note that the first term of (7.14) is identically zero for motions of this form. In the limit  $\eta \rightarrow 1$ , this problem reduces to the spiral Couette problem treated earlier. Our inquiry here is for  $\eta \neq 1$ ; the value  $\eta = 0$ , which corresponds to Hagen–Poiseuille flow, is the physically most interesting case.

To have an exact result for (4.1), (4.2) valid for all  $\eta$ , one notes that for the motion with solid rotation but no differential rotation  $V = 0$ , one can find an exact solution of the problem

$$\rho \ell n^2 = n^2 L u, \quad L^2 \ell + \rho n^2 u = 0, \quad \ell = D \ell = u = 0|_{r=\eta/(1-\eta), 1/(1-\eta)}, \quad (11.1)$$

which arises from (4.1), (4.2). This problem is equivalent to

$$L^3 \ell + \rho^2 n^2 \ell = 0, \quad \ell = D \ell = L^2 \ell = 0|_{r=\eta/(1-\eta), 1/(1-\eta)}, \quad (11.2)$$

and, since  $L\phi + \lambda\phi = 0$  is a Bessel's equation and

$$\phi = A J_n(\lambda^{\frac{1}{2}} r) + B Y_n(\lambda^{\frac{1}{2}} r),$$

we can solve (11.2) with Bessel functions. The exact procedure for finding this solution and the  $\alpha$  analytic perturbation of it is given by Joseph & Carmi (1969).

Given the existence of this energy solution, it is a simple matter to demonstrate, using theorem 1, that the solution also solves the linear problem when the rotation parameters are properly adjusted. To see this, put  $V = 0$  in (6.2) and replace  $\partial/\partial\phi$  and  $\partial/\partial X$  with  $n$  and  $\bar{\alpha}$  to find

$$0 = \text{curl} \{ (1 - (R^2/R_2^2)) U_q \bar{\alpha} \mathbf{u} \} - \mathbf{u} \{ U_q n/R_2^2 + 2\Omega \bar{\alpha} \}.$$

Let  $2\Omega \bar{\alpha} + U_q n/R_2^2 = 0$ ,  $\bar{\alpha} \rightarrow 0$  where  $n$  is the azimuthal periodicity of the energy solution for the given  $\eta$ . For this limit ( $\Omega \rightarrow \infty$ ), the energy and linear eigenvalue problems coincide.

Now we ask, does  $\bar{\alpha} = 0$  give the energy eigenvalue ( $\nu_E$  or  $1/\rho_E$ ) its largest value? This question has been answered affirmatively for Poiseuille motion ( $U_c = 0$ ) of type (2.2) when  $\eta \geq 0.04$ ; but for  $\eta = 0$  (Hagen–Poiseuille flow), the maximizing energy eigenfunction has a spiral form (Joseph & Carmi 1969). We guess that this same result holds for the parabolic profile of form (2.3) and have verified this numerically for  $\eta = 0.2$  (figure 9).

Given that  $\bar{\alpha} = 0$  does give the energy eigenvalue its largest value, we can rigorously exclude sublinear instabilities when  $\bar{\alpha} \rightarrow 0$ ,  $\Omega \rightarrow \infty$ ,  $\Omega \bar{\alpha} \rightarrow -U_q n/R_2^2$ . It is to be expected that, just as for the spiral Couette flow, this result will persist, nearly, if there is also a differential rotation, and the parameters are chosen as in (8.3) and (8.4).

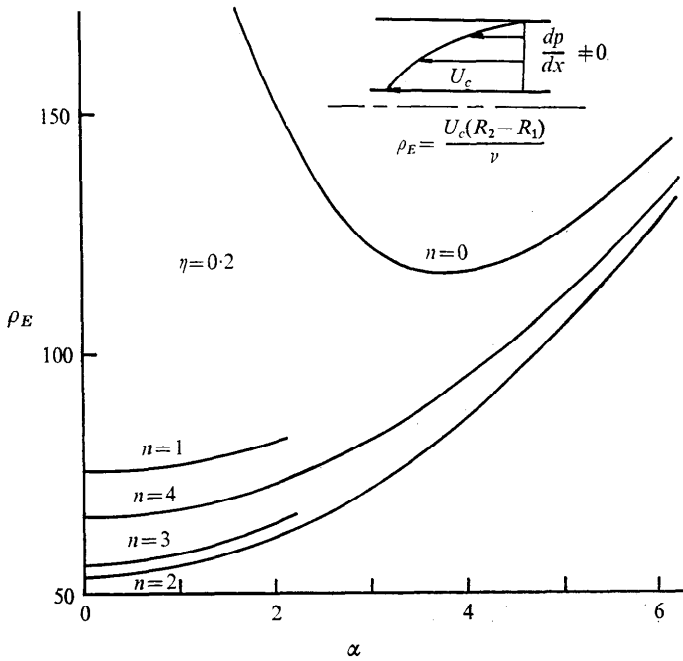


FIGURE 9. Energy result for parabolic profile with  $\eta = 0.2$ . The results of exact numerical integration show that the minimum eigenvalue occurs with wave-numbers  $\alpha = 0$ ,  $\eta = 2$ . Hence, sublinear instabilities are excluded for such flows provided the annulus is rotated rapidly.

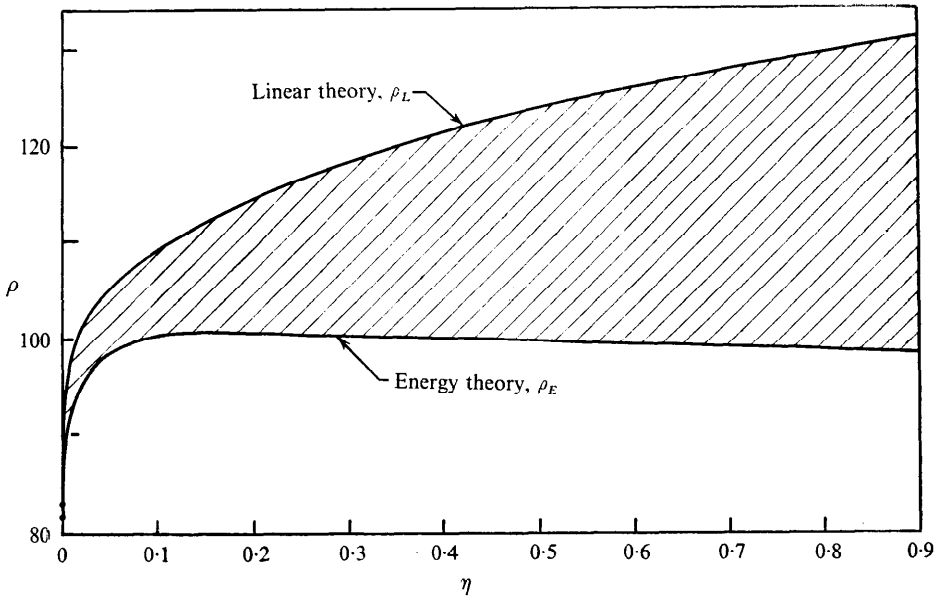


FIGURE 10. Energy and linear stability results for Poiseuille flow in a rapidly rotating annulus. The linear results were obtained by numerical integration of the linear equations for the case of  $\alpha = 0$ ,  $\Omega = \infty$  such that  $\alpha\Omega$  is a finite constant, and the energy results are from Joseph & Carmi (1969). It is seen that a large rigid-body rotation of the annulus forces the linear limit down to the neighbourhood of the energy limit.

The reader will wonder what would be the situation for a true Poiseuille spiral flow ( $U_p \neq 0, U_c = 0$ ). It is not possible for this motion to satisfy (7.11) with  $\eta > 0$ , and one does not expect a close approach between the energy and linear limit. Nevertheless, it remains true that the introduction of rotation even without differential rotation can drop the linear limit by over one order of magnitude and bring the threshold of instability down to energy-like values (Pedley 1969; Nagib *et al.* 1969).

In figure 10, we have given the linear and energy limit, calculated numerically, for rotating Poiseuille flow for  $\Omega \rightarrow \infty$ . The energy limit is independent of  $\Omega$ . Though we cannot make the shaded band smaller, it does confine possible sub-linear instability to a narrow band of Reynolds numbers. The addition of differential rotation would not, we expect, alter this qualitative situation and, in a rough way, equations (8.3), (8.4), which give the values of  $\Omega$  in which the disturbance is steady and the value of  $\Omega_2$  for which the linear and energy limits are closest, could be expected to hold.

A portion of this paper constitutes part of the Ph.D. thesis of B. R. Munson. The work was supported in part by the NSF grant GK-1838 and was completed during the period of a visit by D. D. Joseph to Imperial College made possible by a fellowship from the Guggenheim foundation and the hospitality of the Department of Mathematics.

#### REFERENCES

- CARMI, S. 1970 Linear stability of apial flow in an annular pipe. *Phys. Fluids*, **13**, 829.
- CHANDRASEKHAR, S. 1960 The hydrodynamic stability of inviscid flow between coaxial cylinders. *Proc. Nat. Acad. Sci. U.S.A.* **46**, 137.
- CHANDRASEKHAR, S. 1961 *Hydrodynamic and Hydromagnetic Stability*. Oxford University Press.
- DATTA, S. K. 1965 Stability of spiral flow between concentric cylinders at low axial Reynolds numbers. *J. Fluid Mech.* **21**, 635.
- ELDER, J. W. 1960 An experimental investigation of turbulent spots and breakdown to turbulence. *J. Fluid Mech.* **9**, 235.
- HOWARD, L. N. & GUPTA, A. S. 1962 On the hydrodynamic and hydromagnetic stability of swirling flows. *J. Fluid Mech.* **14**, 463.
- HUGHES, T. H. & REID, W. H. 1968 The stability of spiral flow between rotating cylinders. *Phil. Trans. Roy. Soc. A* **263**, 57.
- JOSEPH, D. D. 1965 On the stability of the Boussinesq equations by the method of energy. *Arch. Rat. Mech. Anal.* **20**, 59.
- JOSEPH, D. D. 1966 Nonlinear stability of the Boussinesq equations by the method of energy. *Arch. Rat. Mech. Anal.* **22**, 163.
- JOSEPH, D. D. 1969 Eigenvalue bounds for the Orr–Sommerfeld equations. Part 2. *J. Fluid Mech.* **36**, 721.
- JOSEPH, D. D. & CARMI, S. 1969 Stability of Poiseuille flow in pipes, annuli, and channels. *Quart. Appl. Math.* **26**, 575.
- JOSEPH, D. D. & SHIR, C. C. 1967 Subcritical convective instability. Part 1. Fluid layers heated from below and internally. *J. Fluid Mech.* **26**, 753.
- KIESSLING, I. 1963 Über das Taylorsche Stabilitätsproblem bei zusätzlicher axialer Durchströmung der Zylindern. *Deutsche Versuchsanstalt für Luft und Raumfahrt*, Bericht 290.

- KIRCHGÄSSNER, K. & SORGER, P. 1968 Stability analysis of branching solutions of the Navier–Stokes equations. *12th Congress of the Int. Union of Theo. and Appl. Mech.*
- KRUEGER, E. R. & DI PRIMA, R. C. 1964 The stability of viscous fluid between rotating cylinders with an axial flow. *J. Fluid Mech.* **19**, 528.
- LUDWIG, H. 1961 Ergänzung zu der Arbeit: ‘Stabilität der Strömung in einem zylindrischen Ringraum’. *Z. Flugwiss.*, **9**, 359.
- LUDWIG, H. 1964 Experimentelle Nachprüfung der Stabilitätstheorien für reibungsfreie Strömungen mit Schraubenlinienförmigen Stromlinien. *11th Int. Congress of Appl. Mech.* 1045.
- MOTT, J. E. & JOSEPH, D. D. 1968 Stability of parallel flow between concentric cylinders. *Phys. Fluids*, **11**, 2065.
- MUNSON, B. R. 1970 Ph.D. Thesis, Dept. of Aerospace Engineering and Mechanics, University of Minnesota.
- NAGIB, H. M., WOLF, L., LAVAN, Z. & FEJER, A. 1969 On the stability of flow in rotating pipes. *Aero Res. Lab. Rep.* 69–0176, *Ill. Inst. Tech.*
- NICKERSON, E. C. 1969 Upper bounds on the torque in cylindrical Couette flow. *J. Fluid Mech.* **38**, 80.
- PEDLEY, T. J. 1968 On the instability of rapidly rotating shear flows to non-axisymmetric disturbances. *J. Fluid Mech.* **31**, 603.
- PEDLEY, T. J. 1969 On the instability of viscous flow in a rapidly rotating pipe. *J. Fluid Mech.* **35**, 97.
- SATTINGER, D. H. 1969 On the linearization of the equations of hydrodynamics. *J. Math. Mech.* **19**, 797.
- SERRIN, J. 1959 On the stability of viscous fluid motions. *Arch. Rat. Mech. Anal.* **3**, 1.
- SERRIN, J. 1968 *Edinburgh Lectures in Fluid Mechanics.*
- SPARROW, E. M., MUNRO, W. D. & JONSSON, V. K. 1964 Instability of the flow between rotating cylinders. *J. Fluid Mech.* **20**, 35.
- YUDOVICH, V. I. 1965 Stability of steady flows of viscous incompressible fluids. *Soviet Physics, Doklady*, **10**, 293.